NAIST-IS-MT0351203

Master’s Thesis

Peak-to-Average Power Ratio Reduction of OFDM Signals Using Carrier Interferometry Codes and Iterative Processing

Khoirul Anwar

February 3, 2005

Department of Information Systems
Graduate School of Information Science
Nara Institute of Science and Technology

A Master's Thesis
Submitted to Graduate School of Information Science,
Nara Institute of Science and Technology
In partial fulfillment of the requirements for the degree of
MASTER of ENGINEERING

Khoirul Anwar

Thesis Committee: Heiichi Yamamoto, Professor
Hiroyuki Seki, Professor
Minoru Okada, Associate Professor

Peak-to-Average Power Ratio Reduction of OFDM Signals Using Carrier Interferometry Codes and Iterative Processing*

Khoirul Anwar

Abstract

Orthogonal Frequency Division Multiplexing (OFDM) is widely believed as the enabling technology for wireless communications due to its high data rates transmission capability and robustness against multipath effects. However, OFDM poses high peak-to-average power ratio (PAPR) problem, as a consequence of independently modulated carriers, that causes low efficiency of the amplifier and increases the complexities of analog-to-digital converter (ADC) and digital-to-analog converter (DAC).

This issue is especially important for mobile terminals to sustain longer battery life time. Therefore, reducing the PAPR can be regarded as an important issue to realize efficient and affordable mobile communication services.

This thesis proposes an efficient PAPR reduction method for OFDM signals by combining the advantages of carrier interferometry (CI) and iterative processing (IP). CI is capable of reducing the probability of high peaks occurrence, however, some of the high peak still remains. Then, iterative processing of clipping is performed to limit these peaks in time domain but the subtraction process hold in frequency domain. The results then confirm that the proposed method is capable of reducing the PAPR significantly, present minimum BER degradation and does not introduce spectrum broadening or out-of-band noise.

Keywords:

OFDM, PAPR reduction, Spreading code, Pseudo-Orthogonal, Carrier Interferometry, Iterative Processing, Spectrum broadening

* Master's Thesis, Department of Information Systems, Graduate School of Information Science, Nara Institute of Science and Technology, NAIST-IS-MT0351203, February 3, 2005.

繰り返し処理とキャリア·インタ-フェロメトリを用いたOFDM信号のPAPRの削減*

Khoirul Anwar

内容梗概

OFDM (Orthogonal Frequency Division Multiplexing) 変調方式は、マルチパスフェージングに強いことや広帯域伝送に向いていることなどから、次世代の無線通信技術として有望視されている。しかし反面、この方式は独立に変調された搬送波が重畳されるために、本質的に信号のピーク電力対平均電力比が高くなるという欠点を有している。その結果、送信増幅器の効率の低下や、アナログ/デジタル変換回路の複雑化を招くなどの問題を生じさせる。この問題はまた、バッテリの耐用時間を短くすることから、特に携帯端末にとって重要である。このような理由から、OFDM信号のPAPRの圧縮は、経済的でかつ使い易い移動通信の実現に極めて重要である。

そこで本研究は、キャリアインタフェロメトリ(CI)と繰り返し処理(Iterative Processing: IP)　技術を利用してOFDM信号のPAPRを効果的に圧縮することを提案している。提案方式ではCI技術によって電力のピーク出現の確率を抑え、IPによって時間領域でピークをクリッピングし、さらに周波数領域で減算処理を行う手法をとる。その結果、提案方式は、BER特性に大きな影響を与えることなく、また信号スペクトルの拡散や帯域外雑音を生じさせることなく、PAPRを大幅に圧縮できることを示すものである。

キーワード

OFDM、PAPR 削減、キャリアインタフェロメトリ、繰り返し処理、クリッピング、スペクトル拡散

*奈良先端科学技術大学院大学情報科学研究科情報システム学専攻修士論文,
NAIST-IS-MT0351203, 2005年2月3日.

To the greatest Parents, who taught me the Value of
Study and Perseverance Ethic…
To my Wife, Azzam and Emiko for the Support of
Spirit and the Patient.

Contents

List of Figures

List of Tables

Chapter 1

Introduction

The demand for high data rate services has been increasing very rapidly and there is no slowdown in sight. Often, these services require very reliable data transmission over very harsh environments. Most of these transmission systems experience many degradations, such as large attenuation, noise, multipath, interference, time variation, nonlinearities, Doppler spread and must meet many constraints, such as finite transmit power and efficient bandwidth. One physical layer technique that has recently gained much popularity due to its robustness in dealing with these impairments is multicarrier modulation.

Unfortunately, one particular major problem with multicarrier signals that is often cited as the major drawback of multicarrier transmissions is its large envelope fluctuation, which is quantified by the parameter called peak-to-average power ratio (PAPR). Since most practical transmission systems are peak-power limited, designing the system to operate in a perfectly linear region often implies operating at power levels well below the maximum power available.

In practice, to avoid operating the amplifier with extremely large back-offs, occasional saturation of the amplifiers or clipping in the digital-to-analog converters must be allowed. This additional process is a nonlinear process which creates inter-modulation distortion that increases the bit-error-rate (BER) in standard linear receivers, and also causes spectral widening of the transmit signal that increases adjacent channel interference to the other users.

This thesis derives a number of relevant results regarding PAPR analysis and proposes a new efficient method, low complexities PAPR reduction algorithm with minimum BER performance degradation and without spectral broadening.

In this method, clipping is introduced to limit the peak-power. However, this clipping process does not introduce spectral broadening, as exists in conventional clipping process, because the subtraction to the original signal is processed in frequency domain instead of in time domain and only affects a minimum BER performance degradation. The clipping process is also done iteratively because zero padding operation in frequency domain causes peak re-growth after converting to the time domain. On the other hand, the given PAPR threshold could not be achieved only in one time iteration. This iterative processing, then, impacts to a little increasing of the calculation amount, but we believe the future digital signal processor (DSP) will do it fast and have no problem on this additional calculation. However, we pay this amount of calculation with our significant PAPR reduction which is about 3 dB with BER degradation is only about 1dB at average BER level of 10^{-4} for QPSK modulation.

1.1 Organization of the Thesis

Chapter 2 introduces peak-to-average power ratio (PAPR) analysis on multicarrier modulation system and more specifically orthogonal frequency division multiplexing (OFDM) and wavelet based multicarrier modulation system (further we called orthogonal wavelet division multiplexing – OWDM).

Chapter 3 presents PAPR reduction technique by exploiting carrier interferometry (CI) codes and pseudo-orthogonal carrier interferometry (PO-CI) codes. Evaluation of this technique is explained in the last section of this chapter.

Chapter 4 evaluates performance of iterative processing (IP) for reducing the OFDM PAPR. The Evaluation was performed on the PAPR and BER performance.

Chapter 5 proposes a new efficient PAPR reduction method for OFDM using the advantage of both CI and IP, called CI/IP method. The structure of transmitter and receiver is introduced and followed by chapter 6 for the performances evaluation of the proposed technique on: PAPR performance, BER performance and also power spectral density analysis. Then, in chapter 7 thesis summary and conclusions are presented.

1.2 Research Contributions

The main contributions of this thesis are the analysis of PAPR for multicarrier modulation (OFDM and OWDM) and the proposal of new method for PAPR reduction. The details of these contributions are listed below by chapter.

Chapter 2: Proves that PAPR problem is also exists on wavelet based multicarrier modulation (OWDM) and we propose the use best spreading code for solving this PAPR problem. The proposed method is superior even with lower load factor or with the oversampled signals.

Chapters 3 and 4: Explains the drawback of PAPR on CI/OFDM when only partial subcarriers number is used for data transmissions. In this chapter, we also clarify that the imperfect orthogonality of PO-CI codes makes this codes only efficient for BPSK modulation and impacts big performance degradation on *M*-QAM modulation. In chapter 4, IP method is evaluated. With this method only, a large amount of calculation and large BER degradation are obtained. Therefore, a new efficient method is required.

Chapters 5 and 6: Proposes a new efficient method for PAPR reduction of OFDM signals by combining the advantage of both CI and IP method. With this proposed method BER performance degradation can be reduced more lowly, spectrum widening can be avoided and of course high PAPR can be reduced significantly by approximately 3dB with QPSK modulation.

Chapter 2

Peak-to-Average Power Ratio on Multicarrier Modulation System

The multicarrier modulation includes a number of transmission schemes whose main characteristic is the decomposition of any wideband channel into a set of independent narrowband channels. Within this family, we focus on Orthogonal Frequency Division Multiplexing (OFDM) and Orthogonal Wavelet Division Multiplexing (OWDM). OWDM which is based on wavelet transform, is still a new technology that has been started a few years ago in 90's, while OFDM which based on Fourier transform has been proposed since 50's.

The main focus of this chapter is to introduce the basic reason of peak-to-average power ratio (PAPR) problem on multicarrier modulation and how to solve this problem with a very simple method. This chapter also provides necessary background for understanding the subsequent chapters.

2.1 Multicarrier Modulation System

Multicarrier technologies are interesting to be studied because of its promise to be capable in transmitting high bit rate. Multicarrier is also robust to multipath fading environment.

All multicarrier modulation techniques are based on the concept of *channel partitioning*. Channel partitioning method then divides the wideband and is spectrally shaped transmission channel into a set of parallel and ideally independent narrowband subchannels. We will focus on discrete time channel partitioning, which partition a discrete time description of the channel. It is assumed that the combined effect of transmit filter, transmission channel and receiver filters can be approximated by finite impulse response (FIR) filter.

Set $\mathbf{h}=[h_0 \cdots h_v]$ the baseband complex discrete time representation of the channel impulse response. The block of output samples $\mathbf{y}=[y_0 \cdots y_{N-1}]$ can be expressed as a function of input samples $\mathbf{x}=[x_{-v} \cdots x_{-1}\, x_0\, x_1 \cdots x_{N-1}]$ and the channel noise $\mathbf{n}=[n_0 \cdots n_{N-1}]$ using the following standard vector representation.

$$\begin{pmatrix} y_{N-1} \\ \vdots \\ y_0 \end{pmatrix} = \begin{pmatrix} h_0 & h_1 & \cdots & h_{v-1} & h_v & 0 & \cdots & 0 \\ 0 & h_0 & h_1 & \cdots & h_{v-1} & h_v & \cdots & 0 \\ \vdots & \ddots & \ddots & \ddots & \ddots & \ddots & \ddots & \vdots \\ 0 & \cdots & 0 & h_0 & h_1 & \cdots & h_{v-1} & h_v \end{pmatrix} \begin{pmatrix} x_{N-1} \\ \vdots \\ x_1 \\ x_0 \\ \vdots \\ x_{-v} \end{pmatrix} + \begin{pmatrix} n_{N-1} \\ \vdots \\ n_0 \end{pmatrix} \tag{2.1}$$

Equation (2.1) can be written compactly as

$$\mathbf{y} = H\mathbf{x} + \mathbf{n} \tag{2.2}$$

for representing the input-output relationship for a single block of samples. In a practical communication system, we may transmit the data in a continuous manner and equation (2.2) become $\mathbf{y}^m = [H\mathbf{x}^m + \mathbf{n}^m]$ where index *m* represents the *m-th* block.

For sending data over a finite-length multicarrier system, the transmitted data must be partitioned into blocks of bits, and each block must be mapped into a vector of complex symbols $\mathbf{X}^m = \left[\mathbf{X}_0^m \cdots \mathbf{X}_{N-1}^m\right]$. The modulated waveform $\mathbf{x}^m$ is expressed as

$$\mathbf{x}^m = \sum_{k=0}^{N-1} \mathbf{m}_k X_k^m = M\mathbf{X}^m \tag{2.3}$$

where $\mathbf{m}_k$ with k={0, …, N - 1} denotes the set of basis vectors in the transmitter (transmit basis vectors) and M is the matrix constructed with the transmit basis vectors as its columns. At the receiver $\mathbf{y}^m$ is the received vectors and demodulated by computing

$$\mathbf{Y}^m = \begin{bmatrix} \mathbf{f}_{N-1}^* \mathbf{y}^m \\ \vdots \\ \mathbf{f}_0^* \mathbf{y}^m \end{bmatrix} = F^* \mathbf{y}^m \tag{2.4}$$

where $\mathbf{f}_k^*$ with k={0, …, N – 1}, denotes the set of basis vectors at the receiver (receive basis vectors) and F* is the matrix constructed with the receive basis vectors as its rows. Then, we can express the overall input-output relationship by

$$\mathbf{Y}^m = F^* HM\mathbf{X}^m + F^* \mathbf{n} \tag{2.5}$$

Different choice for F and M are possible, leading to a number of possible multicarrier structures. Selecting F and M from Fourier transform matrix, obtains OFDM system, whereas selecting F and M from wavelet transform obtains OWDM system. This thesis will focus on both of these multicarrier structures.

2.1.1 OFDM System

OFDM, stands for Orthogonal Frequency Division Multiplexing, has been proposed in the 50’s and with substantial advancement in digital signal processing (DSP) technology now, becoming an important part in the telecommunication area. OFDM has been adopted as a standard for the European wireless data link known as HYPERLAN, as well as adopted in US by well-known IEEE.802.11 and adopted in ISDB-T (Integrated Service Digital Broadcasting for Terrestrial), a standard of Japanese digital television broadcasting system.

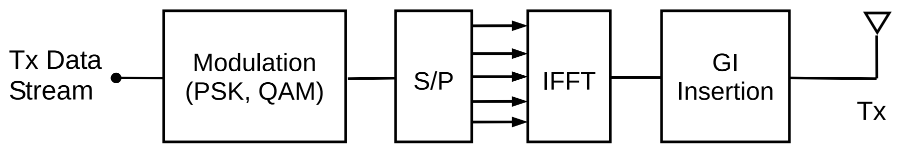

Fig. 2.1 Block Diagram of OFDM transmitter

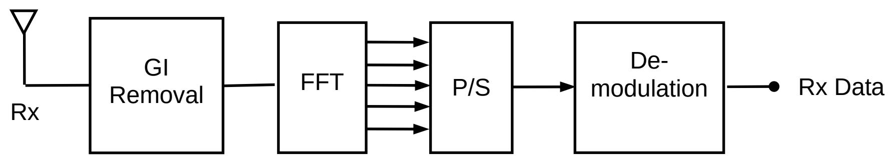

Fig. 2.2 Block Diagram of OFDM receiver

Fig. 2.1 is the block diagram of OFDM transmitter and receiver. An incoming bit stream, most likely with a high bit rate enters a modulation part to be mapped in PSK (BPSK, QPSK), QAM (16QAM or 64QAM) or other modulations. The incoming data symbols then enter a serial to parallel converter, mapping the high data stream into *N* lower-rate (parallel) data streams. Each data stream then placed on its own carrier and carrier spacing is carefully selected to ensure orthogonality i.e. to ensure that carrier can be separable one from another at the receiver side. Next, the carriers are added together. One trick that makes low cost at the transmitter is the use of an Inverse Fast Fourier Transform (IFFT). Then, guard interval (cyclic prefix) is added by copying the last part of the signal to the first part for simplify inter-symbol interference (ISI) mitigation. Finally, this signal, called OFDM symbol, is modulated up to the transmit frequency and then sent out across to the channel.

The benefit of OFDM is best understood when considering the transmission over the channel to against multipath fading. If original high data rate had been sent as it across a single carrier, the wide bandwidth (due to its high bit rate) of the signal would lead to frequency selectivity. Different frequency would experience different gains as they traveled over the wireless channel. As a result, a receiver with a large computational complexity, perhaps one based on equalizer structure would be required.

The OFDM transmitter, as illustrated in Fig. 2.1 simplifies the channel effects. In OFDM, high data rate is not sent as it is, but rather serial to parallel converted prior to the transmission. This leads to N channels low-rate data stream, each demonstrating a narrow bandwidth and sent out on its own carrier. As a result, when sent over the channel, each low-rate data stream experiences a flat fade, i.e. the gain is constant over the all frequencies. Here no equalizer structure is required at the receiver.

The receiver structure is described in Fig. 2.2. The incoming symbol stream is first returned to the baseband by use of an appropriate mixer. Next, guard interval is removed and the incoming symbol stream separated into its N low-rate data stream by the use of FFT. Once symbol stream has been separated from one from another, a simple decision device is applied. Demodulation process then performed and recovered high bit rate is obtained.

2.1.1 OWDM System

Recently, a new class of multicarrier system based on wavelet transform has been proposed [1] and for simplicity, called OWDM in this thesis. OWDM, stands for Orthogonal Wavelet Division Multiplexing, shares all the benefit of OFDM and exhibits further benefit such as higher efficiency due to elimination of guard interval (GI). It is considering on wavelet waveforms which are well localized both in time and frequency domain, while sinusoid waveforms, are only localized in frequency but not in time domain. Thus, time domain diversity of sinusoid waveform within one symbol period is difficult to achieve. Therefore, a guard interval (GI) is needed to eliminate residual Inter Symbol Interference (ISI). This addition of GI signals, then introduces overhead that decreases bandwidth efficiency.

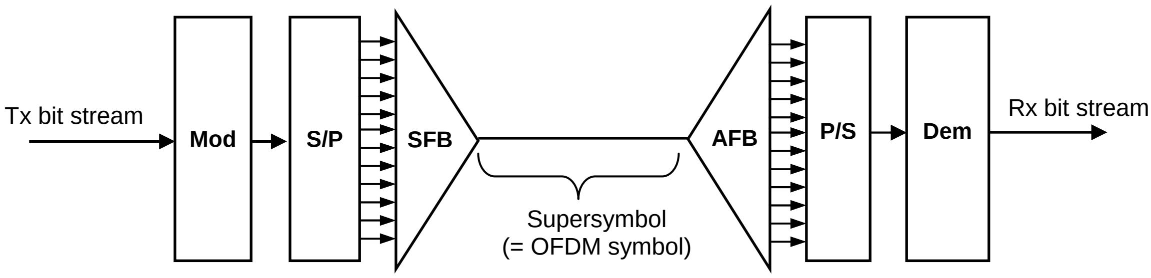

Fig. 2.3 A Generic OWDM Transceiver

Fig. 2.3 illustrates a generic block diagram of OWDM transceiver, while the details are then shown in Figs. 2.4 and 2.5. OWDM system employs two filter bank i.e. synthesis filter bank (SFB) placed at the transmitter side and analysis filter bank (AFB) placed at the receiver side. SFB has the same function as IFFT, while AFB (analysis filter bank) has the same function as FFT in OFDM system. The detail explanation about filter bank is in [2] and [3].

As described in Fig. 2.3, modulated data in PSK or QAM are inputted to the SFB to generate the multicarrier signal, and then transmitted over the transmission medium (wireline or wireless). Received signals corrupted by additive white Gaussian noise (AWGN) and fading is received by AFB, demodulated and converted back to serial-sequence for recovering the transmitted data. Compared to the existing DFT-based system, we can adjust the subband or subcarrier overlapping in the structure of SFB-AFB (then called transmultiplexer [2]) by controlling the wavelet filter in each subband. This flexibility of the design is one of the advantage contributions of OWDM.

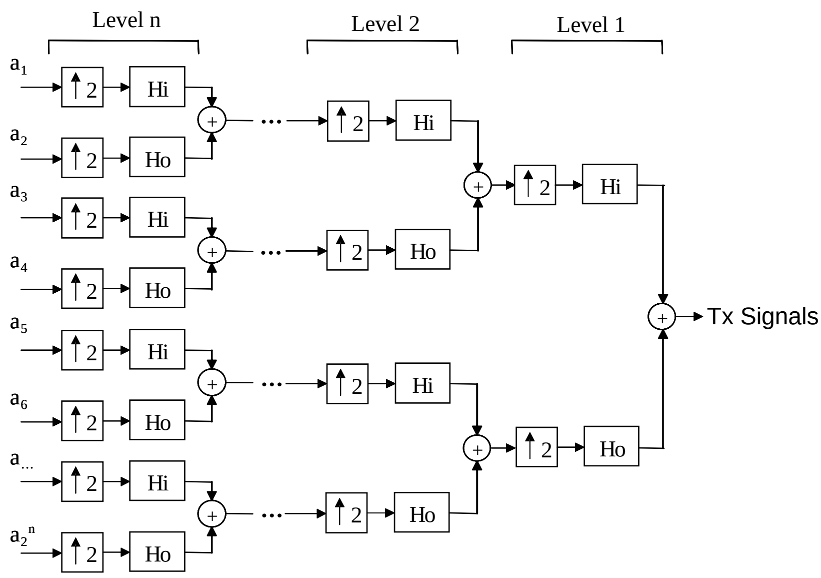

Fig. 2.4 Synthesis Filter Bank (SFB) at the Transmitter Side

Figs. 2.4 and 2.5 show the detail structure of a transmultiplexer with the number of input and output are an power of two (2^n) where n is the number of stages. Wavelet filters $\mathbf{H}_i$ is as high pass filter (HPF) and $\mathbf{H}_o$ as low pass filter (LPF) at the transmitter, while $\mathbf{H_i}$' and $\mathbf{H}o$' are as HPF and LPF respectively at the receiver. All filters should be designed so that the occurred aliasing are exactly cancelled out. This condition leads to the construction of perfectly reconstruction (PR) filter bank, which is called quadrature mirror filter (QMF). Considering the carrier allocation which is divided into 2^n subcarriers or subbands, the symbol a_1 is the symbol with the highest frequency, while symbol a_{2^n} is the symbol with the lowest frequency among all of the transmultiplexer subbands. Upsampling is performed at the transmitter before entering filter in its stage, and downsampling is held at the receiver after each data passed a filter of its stage.

In this thesis, $\mathbf{H}_i$, $\mathbf{H}_i$', $\mathbf{H}_o$, and $\mathbf{H}_o$' are selected from the filter which is provided by Haar wavelet. Haar wavelet is selected due to its simplicity in design and calculation. Haar wavelet then confirms that $\mathbf{H}_i = [1 \quad -1]$, $\mathbf{H}_o = [1 \quad 1]$, $\mathbf{H}'_i = [-1 \quad 1]$ and

$\mathbf{H}'_o = [1 \quad 1]$. For example, let's consider OWDM with 2 stages, 4 subcarriers, assume data input is [0 0 1 0], let's take a_3=[1], while $a_1 = a_2 = a_4$ = [0]. Filter for this data will be H_i and H_o (other filter results zero), after first upsampling the output is [0 1 0] then convoluted with H_i resulted [0 1-1 0]. The second upsampling's output is [0 0 1 0 -1 0 0], convolution with Ho resulted [0 0 1 1 -1 -1 0 0], then the Tx signal is only [1 1 -1 -1]. The summation process is ignored because other data are zeros.

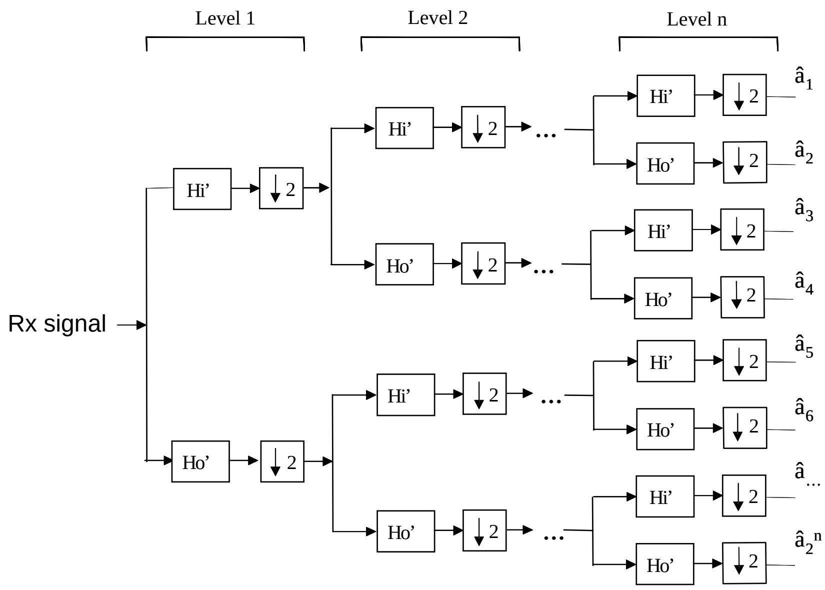

Fig. 2.5 Analysis Filter Bank (AFB) at the Receiver Side

Tx signal then received at AFB as described in Fig. 2.5. The filter path for this received signal is Ho' → Hi', as the inverse of filter sequence at the transmitter Hi → Ho. Result of convolution with Ho' is [1 2 0 -2 -1], then downsampled and becomes [2 -2]. The convolution with Hi' resulted [-2 4 -2] and downsampled becomes [4], and then normalized with 4, obtained [1] at subcarrier a_3. Total received data is then [0 0 1 0], which is the same with the transmitted data. This simple example shows that SFB and AFB are not complex when compared to IFFT/FFT matrix. This is one advantages of OWDM system in reducing the complexities.

2.2. Peak-to-Average Power Ratio (PAPR)

One particular problem with multicarrier signals, which is often cited as major drawback of multicarrier system is its large envelope fluctuations, which is usually measured by parameter called PAPR. PAPR is defined as the ratio of the peak instantaneous power and the average power i.e., mathematically expressed as

$$PAPR = \frac{\max_{0<t<T_s} |s(t)|^2}{\text{mean}_{0<t<T_s} |s(t)|^2} \tag{2.6}$$

where s(t) is multicarrier symbol with interval $0<t<T_s$. It means that this PAPR is evaluated per OFDM symbols. Throughout this paper, all PAPR is calculated per multicarrier symbol e.g. OWDM symbol and OFDM symbol.

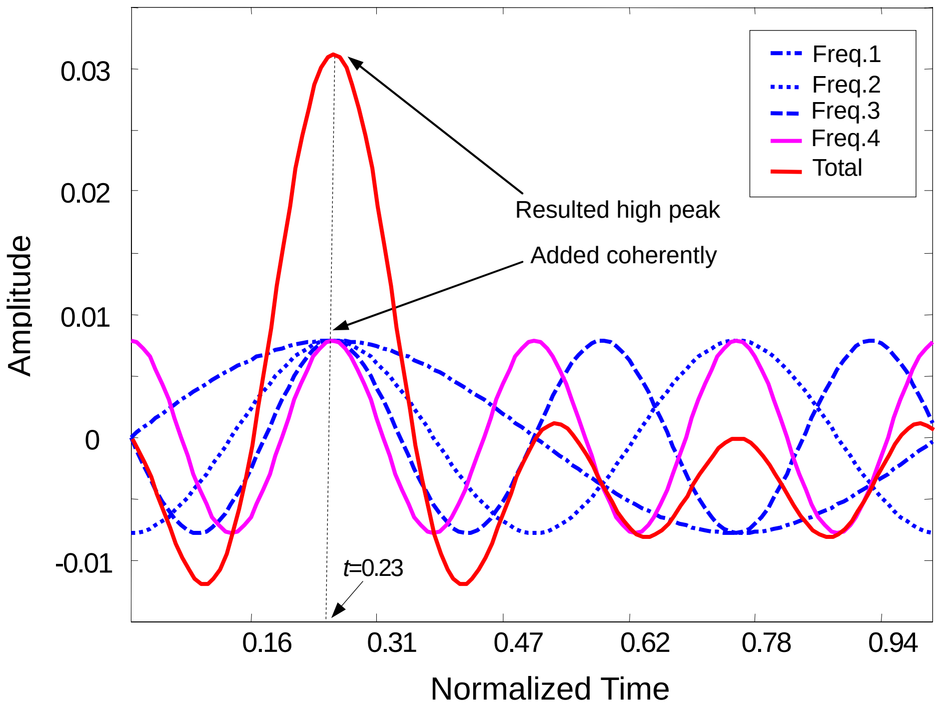

Fig. 2.6 High Peak Appearance on Multicarrier System

Fig. 2.6 illustrates how a coherent superposition among modulated carrier results a high peak. Signal with frequency *Freq.1* (the lowest), *Freq.2*, *Freq.3* and *Freq.4* (the highest) have the same peak and phase at time t=0.23. Multicarrier signal is obtained from the summation of these signals which results in a new signal with high peak of approximately four times compared to individual signal. PAPR is then calculated from the ratio of this instantaneous peak power and average power of this multicarrier signal.

It is also important to note that throughout this thesis, PAPR will only refer to the baseband PAPR, because PAPR in the passband depends on the PAPR in baseband and approximately twice (3dB). A simple calculation is described as below, suppose that carrier frequency is f_c, then

$$\begin{aligned} s_{PB}(t) &= \mathrm{Re}\{s(t)e^{j2\pi f_c t}\} \\ &= \mathrm{Re}\{s(t)\}\cos(2\pi f_c) - j\,\mathrm{Im}\{s(t)\}\sin(2\pi f_c t) \\ &= S_I(t)\cos(2\pi f_c t) - jS_Q(t)\sin(2\pi f_c t) \end{aligned} \tag{2.7}$$

since carrier frequency is usually higher than the signal bandwidth, i.e. $f_c >> N/T_s$ (N is subcarrier number), then from (2.7), the maximum modulated signal is the same as the maximum of baseband signal, i.e.,

$$\max|s_{PB}(t)| \approx \max|s(t)| \tag{2.8}$$

For QAM modulation $\mathrm{mean}|s_I(t)|^2 = \mathrm{mean}|s_Q(t)|^2 = \frac{1}{2}\mathrm{mean}|s(t)|^2$, so from (2.7) the average power for QAM can be written

$$\mathrm{mean}|s_{PB}(t)|^2 = \frac{1}{2}\mathrm{mean}|s_I(t)|^2 + \frac{1}{2}\mathrm{mean}|s_Q(t)|^2 = \frac{\mathrm{mean}|s(t)|^2}{2} \tag{2.9}$$

It is clear that from (2.8) and (2.9), the passband PAPR is approximately twice (3dB higher) than the baseband PAPR, i.e.

$$PAPR\{s_{PB}(t)\} = \frac{\max|s_{PB}(t)|^2}{\text{mean}|s_{PB}(t)|^2} = \frac{\max|s(t)|^2}{\text{mean}|s(t)|^2 / 2} = 2PAPR\{s(t)\} \tag{2.10}$$

2.2.1. PAPR Performance of OFDM System

Suppose average power of OFDM is $P_{mean} = NP_0$, where P_0 is the power on one carrier, i.e. $P_0 = \frac{1}{2}A^2$, in the worst scenario when N carrier combine coherently, OFDM peak's power is equal to:

$$P_{\max,worstcase} = \frac{1}{2}\left(\sum_{i=1}^{N} A\right)^2 = \frac{1}{2}(NA)^2 = \frac{1}{2}N^2A^2 \tag{2.11}$$

so PAPR on the worst case can be expressed as

$$PAPR_{worstcase} = \frac{N^2 P_0}{NP_0} = N \tag{2.12}$$

Practically it rarely occurs and with equation (2.6), PAPR for OFDM signals is performed by computer simulation and plotted in Fig. 2.7. Though, this figure shows that the increasing in PAPR is linear to the increasing in subcarriers numbers, but this PAPR is not equal to the number of subcarriers (N). Take an example (N=64, Ts=250 μsec), although maximum PAPR is $10\log_{10}(64)$=18dB, only once every 2.5 minutes (10^4 x 250 μsec), the PAPR of OFDM exceeds $10\log_{10}(12)$=10.79dB.

Thus, the often quoted PAPR value of N for multicarrier signals is extremely pessimistic for appropriately randomized data. Although the PAPR for practical system is below 12-15dB most of the time, this value is still high and PAPR reductions are still of great interest. There are many different alternatives solution to this, and two methods will be summarized in chapters 3 and 4. The subsequent chapters (5 and 6) are devoted to our novel method for reducing PAPR in OFDM signals.

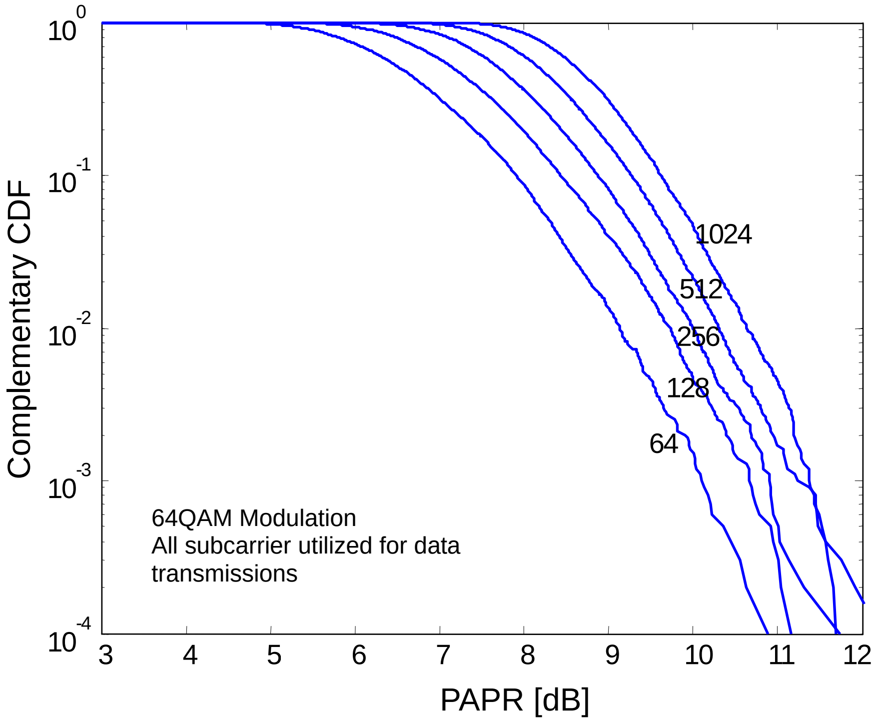

Fig. 2.7 PAPR Performance of OFDM System

Throughout this thesis, we will evaluate PAPR in dB (decibel) on x axis and CCDF (Complementary Cumulative Distribution Function) on y axis. The symbol CDF of $PAPR\{s(t)\}$ is

$$
\begin{aligned}
\mathrm{Prob}\{\mathrm{PAPR}\{\mathrm{s(n)}\} < \gamma^2\} &= \mathrm{Prob}\left\{\frac{|s(0)|^2}{\mathrm{mean}|s(n)|^2} < \gamma^2, \frac{|s(1)|^2}{\mathrm{mean}|s(n)|^2} < \gamma^2, \cdots, \frac{|s(N-1)|^2}{\mathrm{mean}|s(n)|^2} < \gamma^2\right\} \\
&= \left(\mathrm{Prob}\left\{\frac{|s(n)|^2}{\mathrm{mean}|s(n)|^2} < \gamma^2\right\}\right)^N \\
&= (1 - 2Q(\gamma))^N
\end{aligned}
\tag{2.13}
$$

Thus, the complementary CDF becomes $CCDF = 1-(1-2Q(\gamma))^N$, where N is subcarriers number and γ is the observed PAPR level. As a conclusion of describing PAPR using CCDF, it can be inferred from Fig. 2.7 that on CCDF of 10^{-3} OFDM PAPR is not more than 10dB with 64 subcarriers and not more than 13dB for 1024 subcarriers.

2.2.2. PAPR performance of OWDM System

Fig. 2.8 shows the original PAPR of OWDM system without any reduction technique. In this figure, the PAPR of OFDM system is redrawn in the same graph. It is easy to see that PAPR of OWDM is rather similar to that of OFDM system, even there is a little different case (OWDM is better), but as reported in [4][5], the difference is too small and possible to be neglected. The difference is by about 0.3dB only on CCDF of 10^{-3} or 10^{-4}.

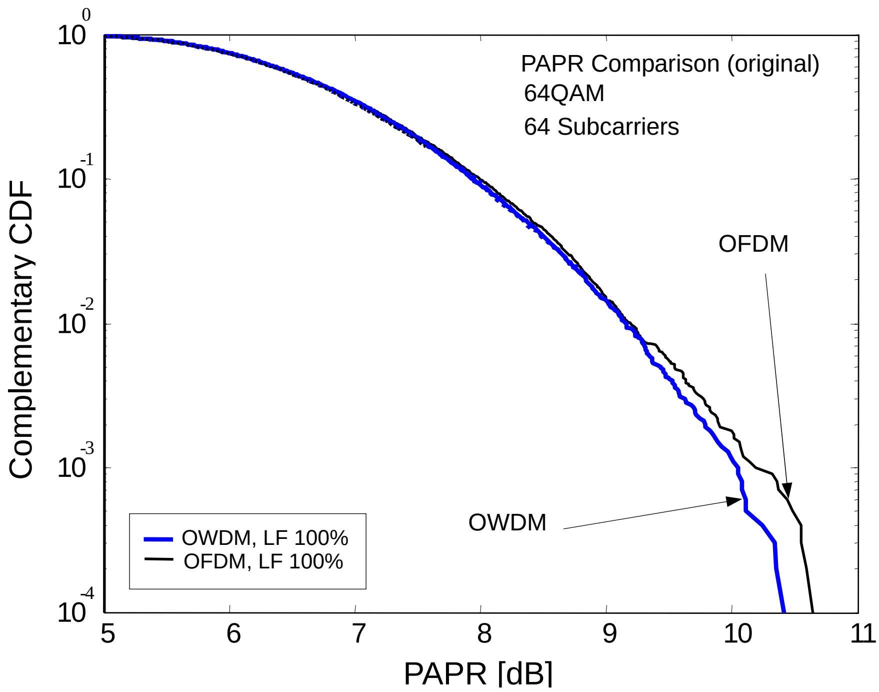

Fig. 2.8 PAPR Performance of OWDM System (Compared to OFDM System)

However, from figures 2.7 and 2.8, it can be concluded that 99.99% of the OFDM and OWDM symbols have PAPR $\leq$ 12dB (16) << N, and statistically, PAPR does not increase significantly with increased N. It leads us to introduce an efficient method for PAPR reduction for both of OFDM system and OWDM system.

2.3 Technique for PAPR Reduction

It is difficult to classify all the effort for reducing PAPR for multicarrier data transmission. The following is probably the most commonly accepted classification of many PAPR reduction techniques. At the higher level this classification divides the methods into PAPR reduction with distortion and PAPR reduction without distortion (distortionless). In the first set of techniques, the transmitter is not designed for the maximum PAPR range and transmit symbols are distorted. These methods degrade the decoded bit-error-rate (BER) and more described in section 2.3.1. The latter methods reduce the symbols PAPR prior to the nonlinear device with-out increasing the BER. These methods are described in section 2.3.2 and typically achieve lower PAPR at expense of a reduced data rate.

2.3.1 PAPR Reduction with Distortion

Probably the simplest way to reduce the PAPR of OFDM/OWDM transmit sequence is to clip the signal at the transmitter to the desired level. This operation can be implemented to the discrete samples prior to the DAC or by designing the DAC and/or amplifier with saturation level which are lower than the dynamic range. This approach is widely used although it is known to degrade the received BER and to increase out-of-band radiation (spectrum broadening). Detail analysis on this effect is analyzed in [4][5].

Some method can avoid spectral broadening problem, unfortunately none of them mitigates the BER increases for a general channel. This increase in BER can be corrected with error correcting codes, but an expense of a reduction in the effective data rate (low efficiency), an increased complexity at both the transmitter and receiver end increase the overall delay of latency of the system. In chapters 5 and 6, we describe a new clipping technique without spectral widening and minimum BER performance.

2.3.2 PAPR Reduction without Distortion

This method reduces the PAPR prior to the nonlinear device without increasing of BER. There is a number of structure phase vectors that generate low PAPR multicarrier symbols. Generally this method can be achieved by employing some orthogonal coding technique that has capability of reducing the peak. In [6], carrier interferometry (CI) code is introduced to be an excellent code for obtaining low PAPR without BER performance degradation, spectral splatter and no loss in bandwidth.

Our proposed technique for reducing the PAPR for OWDM system in the next section (section 2.3.3) can be classified to the second classification, by employing spreading codes that has a similarity with the modulator. PAPR reduction for OFDM signals is then proposed by combining both of with and without distortion.

2.3.3 Proposed PAPR Reduction Method for OWDM System

Our method is one of the PAPR reductions without distortion due to no distortion is introduced. We introduce appropriate wavelet domain spreading code similar to that of proposed in [6], and resulting in a new OWDM system with spread spectrum. We consider the employing of Haar wavelet due to its simplicity both in simulation and implementation.

Comparison with other codes is also presented, for making sure that our proposed code is truly capable of reducing the PAPR significantly. These codes were selected considering the orthogonality properties, i.e. Golay complementary, carrier interferometry (CI) and Hadamard code. Carrier interferometry has been reported to exhibit significant low PAPR of OFDM [6] by about 5 dB lower than the original on cumulative distribution function (CDF) of 99.99%. However, investigating with oversampling process, the reduction is only by about 2 dB lower than the original. It means many peaks were undetected in case of without oversampling. The detail of CI with OFDM will be discussed in chapters 3, 5 and 6.

Considering the wavelet based MCM system (further simplification become OWDM), Hadamard spreading code exhibits low PAPR among others, though PAPR investigation with oversampling is employed. Hadamard code is capable of keeping the PAPR by about 5dB lower than the original, both with and without oversampling. It becomes an excellent code in combining with Haar wavelet, because usually, performance with other code decreases when oversampling process is utilized. In this thesis, we also show the secret reason of Hadamard code in attaining low PAPR by illustrating the transmitted signal envelope of Hadamard and CI for the comparison.

New OWDM with Spreading Code

Fig. 2.9 illustrates the proposed spreading technique for OWDM with K orthogonal subcarriers and N number of users [7][8]. For data modulation, the 64QAM is used. Converted data in parallel are then multiplied by orthogonal spreading code ($C_n(K)$) with length K defined in the wavelet domain to obtain diversity benefits. As illustrated in Fig. 2.9(a), multiplied symbols are then summed through all of the users to obtain new generated symbols, and then inputted to the SFB. The outputs of SFB are then transmitted as the transmitted signals. These signals are then called as OWDM symbol or supersymbols as used in [2] (it corresponds to OFDM symbol in OFDM system).

Transmitted signals may be corrupted by additive white Gaussian noise (AWGN) and fading effects which may destroy the orthogonality properties. PR filters alone inside SFB and AFB are not so strong to recover the data. An equalization technique for OWDM system was then required [1]. At the receiver illustrated in Fig. 2.9(b), received signals are then despread-ed and summed to obtain data that is the same as the original.

Considering the computer simulation, assumed parameters are presented in Table 2.1. All data are modulated using 64QAM, and transmitted over AWGN channels. With

64 subcarriers, spreading codes length designed to have length equal to 64. In this section, we demonstrate the PAPR performance of both OWDM and OFDM systems originally without any reduction techniques, and then we reduced the PAPR and measured with various load factors, oversampling process and amplitude limitation conditions.

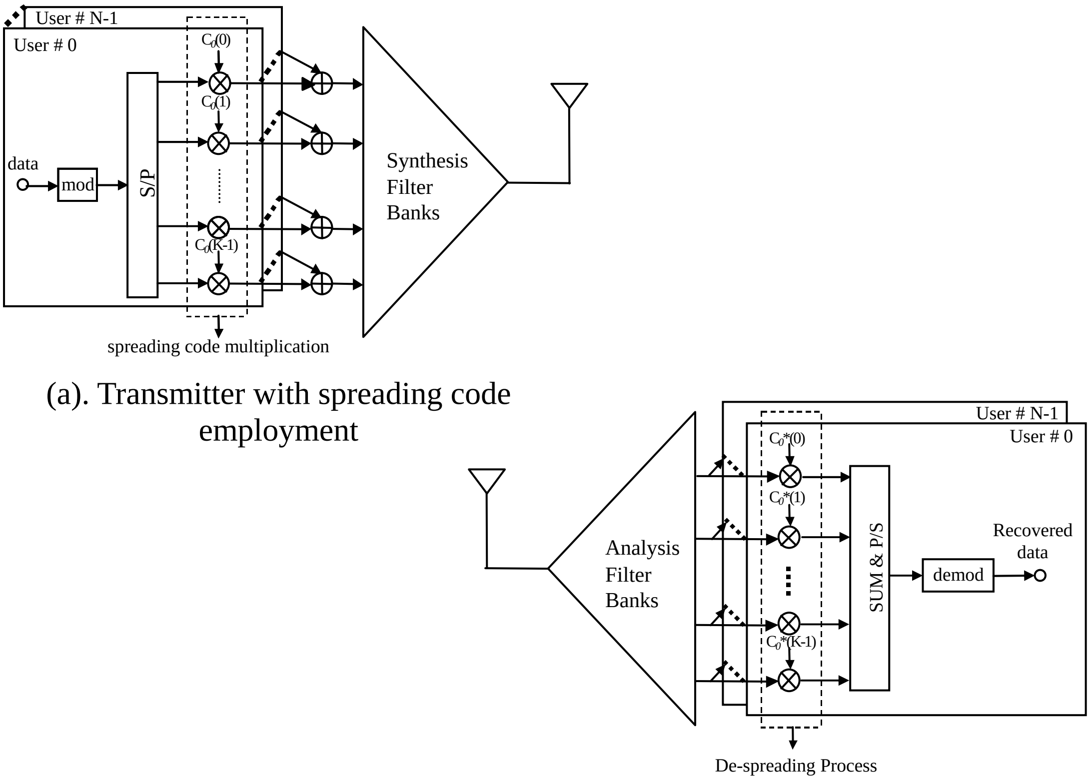

(a). Transmitter with spreading code employment

(b). OWDM receiver with De-spreading process

Fig. 2.9 Proposed New Model of OWDM with Spreading Code

Reduction by the use of Spreading Codes

As mentioned above, we selected spreading codes based on the good orthogonality properties and capability to eliminate the effect of inter-symbols interference (ISI). These codes are Hadamard, carrier interferometry (CI) and Golay complementary.

TABLE 2.1

SIMULATION PARAMETERS FOR OWDM SYSTEM

Transmitter	Modulation	64QAM
	Spreading Code	Hadamard, Carrier Interferometry, Golay Complementary
	Number of Subcarriers	64
	FFT Point	64
	Load Factor	50%, 75%, 100%
Channel	AWGN	
Receiver	Channel Estimation	Off
	Equalization	Off

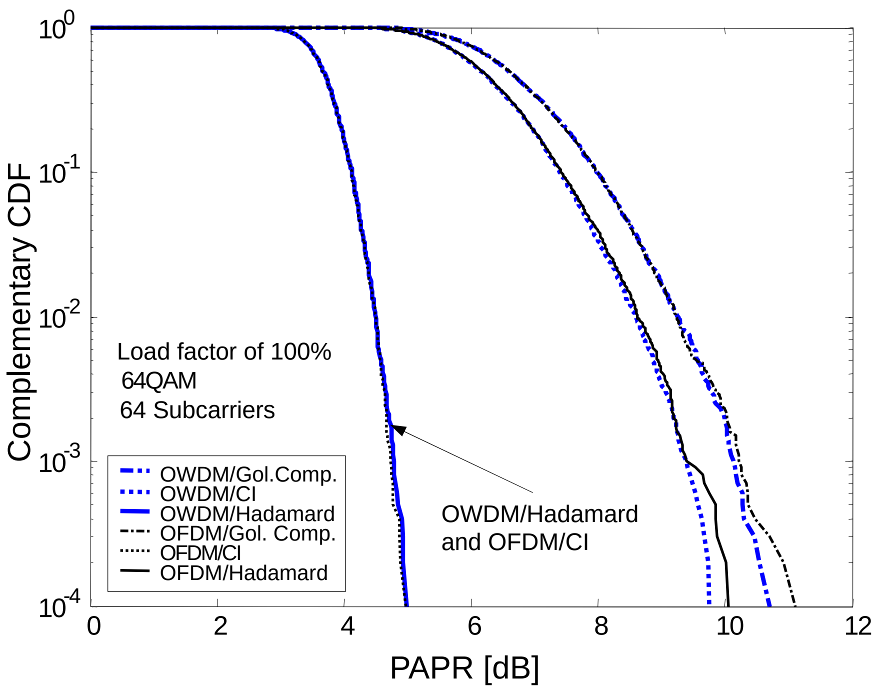

Fig. 2.10 OWDM PAPR Performance for Load Factor of 100%

PAPR shown in Fig. 2.10 are that of OWDM and compared to the PAPR of OFDM system. With load factor of 100% as in Fig. 2.10, the lowest PAPR is achieved with Hadamard, while in OFDM is achieved by CI. This PAPR reduction values are completely similar i.e. by about 5 dB on CDF of 99.99%.

For an advanced performance evaluation of the codes, we examine the PAPR with variation of load factors. It is because some codes contributes a significant reduction only when load factor is high, but different result when load factor is less than 100%. PAPR performance with load factor of 75% and 50%, are then plotted in Fig. 2.11 and Fig. 2.12 respectively.

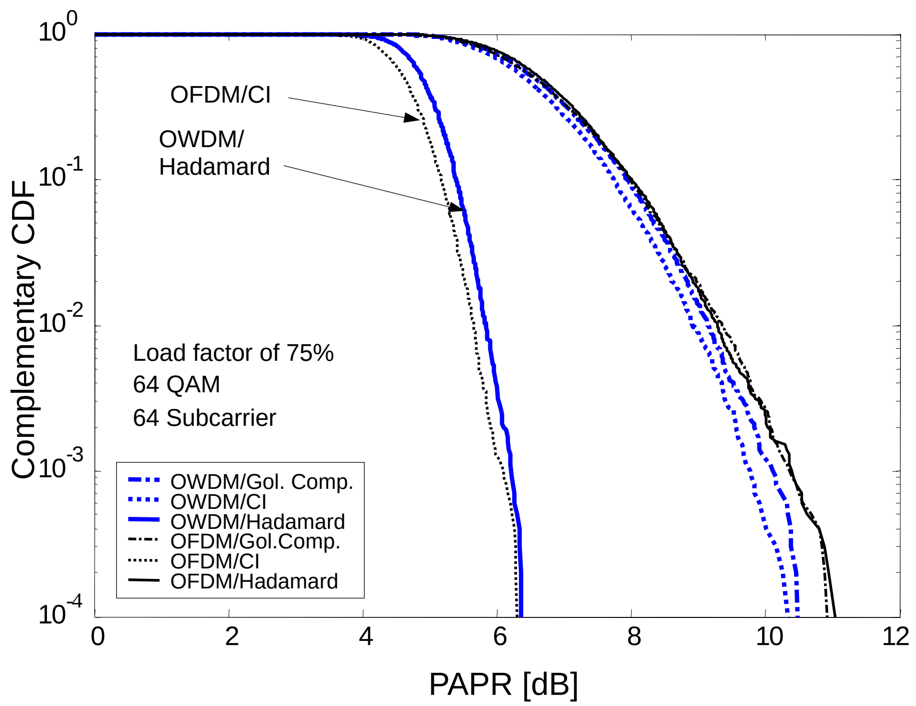

Fig. 2.11 OWDM PAPR Performance for Load Factor of 75%

Load factor, which corresponds to the number of active users, impacts significantly to the performance of PAPR. With load factor of 100%, PAPR OWDM/Hadamard and OFDM/CI is about 5 dB. Then, It increased with the decreasing of the load factor, become 6.3 dB when load factor is 75% and 8.5 dB when the load factor is 50%. Both are with the perfect similarity properties, due to its capability to avoid superposition of signals in each transmitted supersymbol. Golay complementary and CI in OWDM, also Hadamard and Golay complementary in OFDM are not capable of reducing PAPR event small.

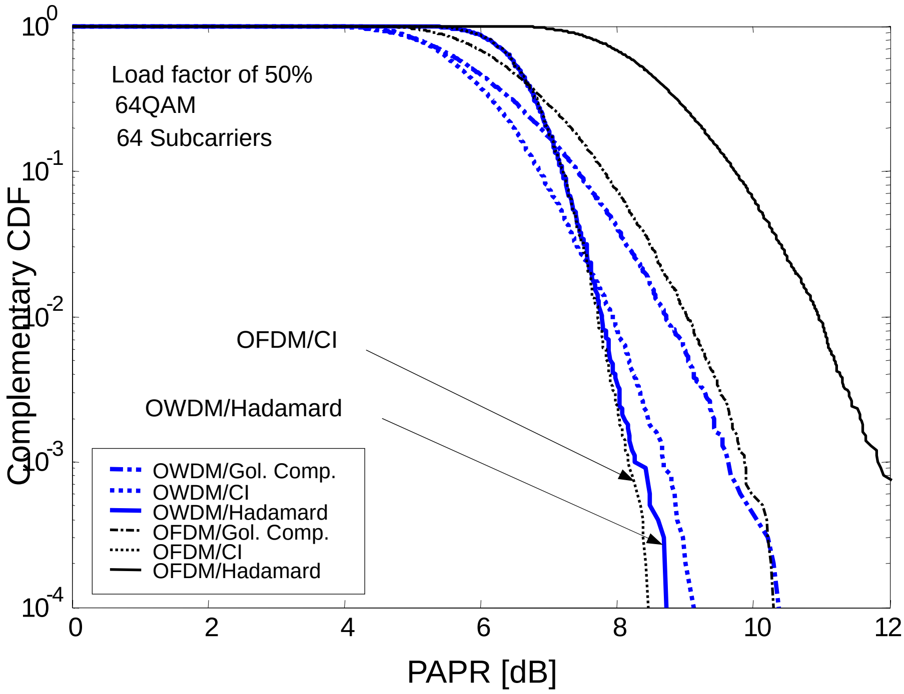

Fig. 2.12 OWDM PAPR Performance for Load Factor of 50%

Performance with Oversampling

Since the PAPR performances are closed to the evaluation of continuous signal rather than digital signal (with small sampling), the true conditions of PAPR evaluation should be approached by oversampling. Therefore, in this section we discuss the performance in case of evaluation with oversampling process employed.

In this thesis, we consider to use the oversampling factor (*J*) of 4, because the value more than 4 does not give significant impacts, so this value is good enough for representing a continuous signal. It means that with original 64 samples, let $A_{origonal}=\{A_0, A_1, \ldots A_{63}\}$, $(J\text{-}1)*64$ of zeros are then inserted and the results with 256 samples become $A_{oversampling}=\{A_0, A_1, \ldots A_{64}, 0_1, 0_2, \ldots 0_{191}\}$. The final results for various load factors of 100%, 75% and 50% are then plotted in Figs. 2.13, 2.14 and 2.15 respectively.

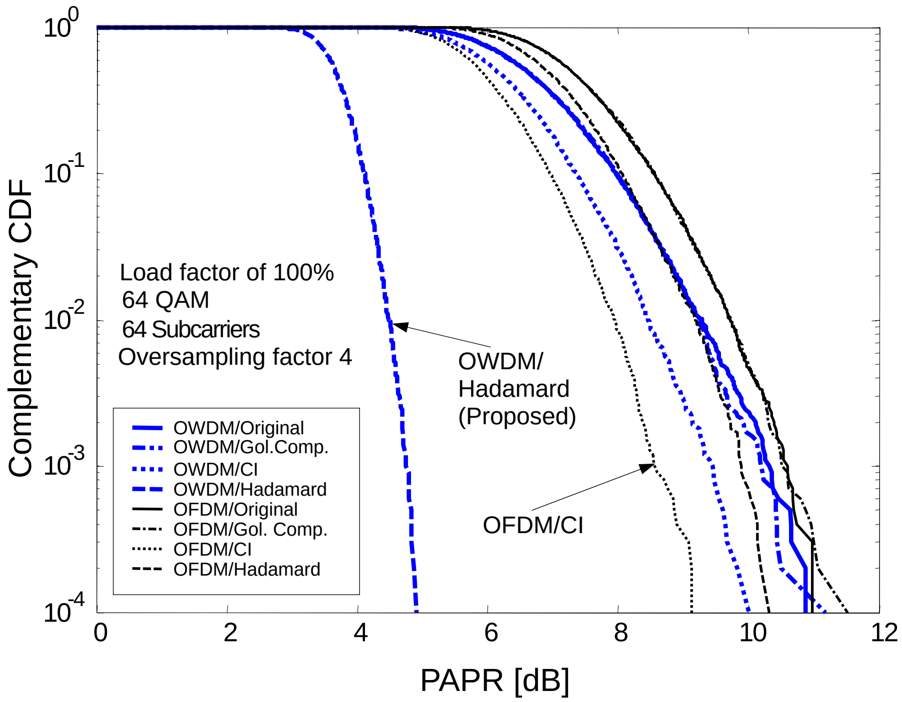

Fig. 2.13 OWDM PAPR Performance with Oversampling for Load Factor of 100%

Fig. 2.13 shows PAPR characteristic with Hadamard code on OWDM system has the minimum PAPR among others. OWDM/Hadamard PAPR is not affected by oversampling process in this case, while OFDM/CI increase from 5dB without oversampling (Fig. 2.10) become approximately 9 dB in Fig. 2.13. It means that many points have been undetected when oversampling J=1, and the peaks appear when we put J=4.

In Fig. 2.14, PAPR of OWDM/Hadamard increased approximately 1.5dB from 5dB to 6.5dB. However, it is still the lowest among others. PAPR of OFDM/CI also increased by about 1.5dB from 9dB to 10.5dB. Golay Complementary does not introduce any good performance both of in OWDM and OFDM system. Comparing to Fig. 2.11, we can conclude that with load factor of 75%, PAPR of OWDM is similar. This condition is not affected by the effect of oversampling.

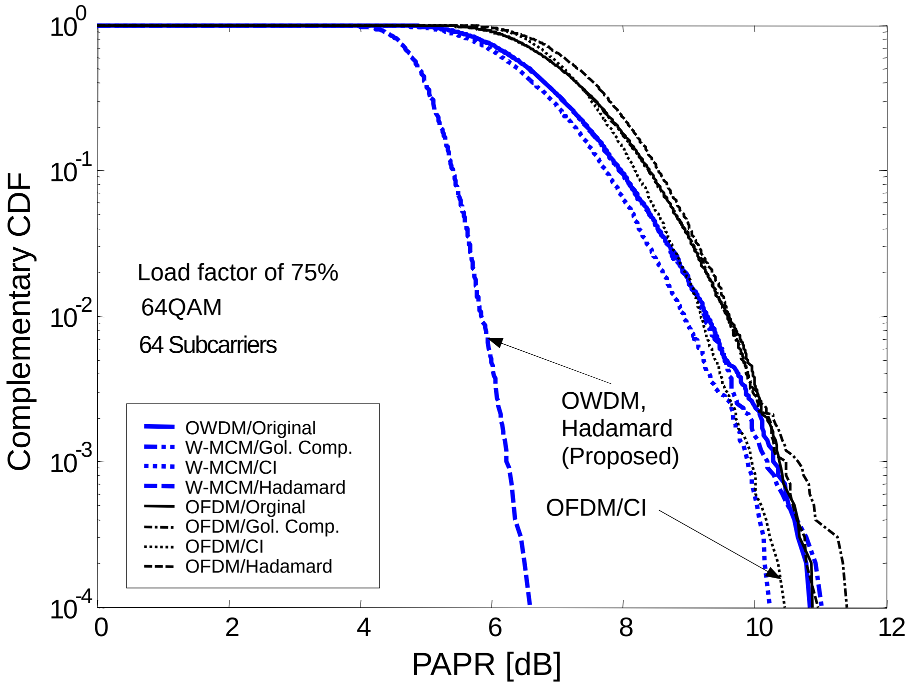

Fig. 2.14 OWDM PAPR Performance with Oversampling for Load Factor of 50%

Continuing the analysis with lower load factor of 50% as presented in Fig. 2.15, PAPR of OWDM/Hadamard increased by about 2dB, from 6.5dB to 8.5dB, 2dB below the original PAPR of OWDM system. However, performance of OFDM with CI increased more higher, from 10.5dB up to 12dB. In this case, the PAPR of OFDM without any spreading code is better.

As the conclusion about oversampling effects, it can be concluded that OFDM/CI code could not keep the PAPR level lower, while OWDM/Hadamard is capable of holding the PAPR at a lower level, and independent of the case of with oversampling or without oversampling. As general conclusion for Golay Complementary, this code could not give any contribution to the reduction of OWDM PAPR and OFDM PAPR. The results of with and without oversampling are quite similar with this code.

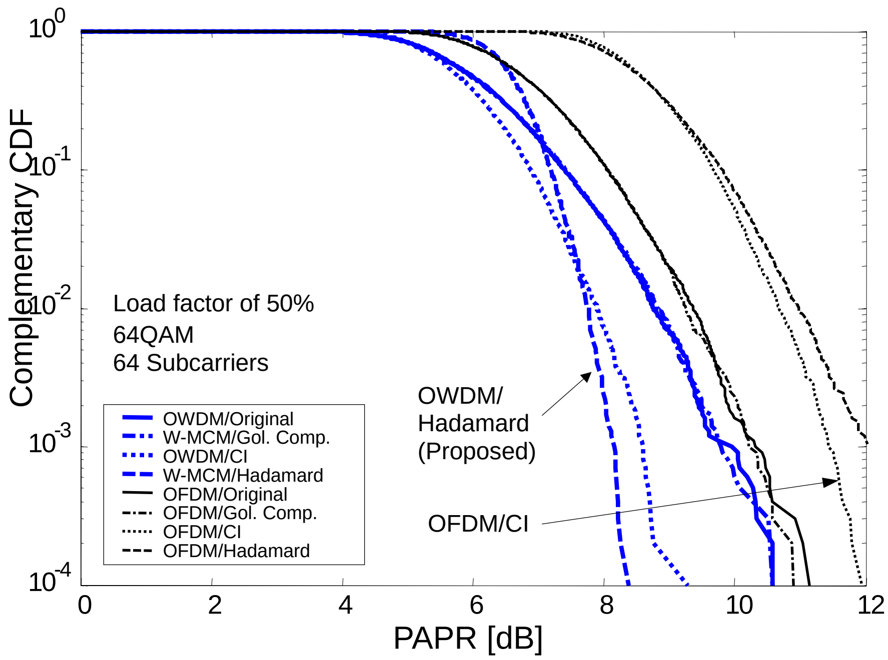

Fig. 2.15 OWDM PAPR Performance with Oversampling for Load Factor of 50%

Performance with Amplitude Limitation

The peak of transmitted signal should be same or below the maximum level of linear region in the amplifier due to distortion effect of nonlinear region. The simplest way to deal with this evaluation is clipping or limiting the peak of transmitted signals with a soft limiter (without phase noise). However, bit error rate (BER) will increase on the account of the distortion effect. The more we clip the larger data loss.

BER was investigated with 64QAM modulation, 64 subcarriers and AWGN as the channel model with load factor assumed 100%. Clipping level was demonstrated by clipping ratio (CR) as in [4], which is mathematically defined in (3), where *A* is the maximum amplitude after clipping and σ is the rms level of wavelet based MCM signal before clipping in one supersymbol. Relation of CR, A and σ is shown as equation (3).

$$CR = \frac{A}{\sigma} \tag{2.14}$$

The simple receiver design for this system has been presented in Fig. 2.9 (a) and (b). We assume no multipath fading effect and therefore this receiver design is sufficient enough to demonstrate the BER performance.

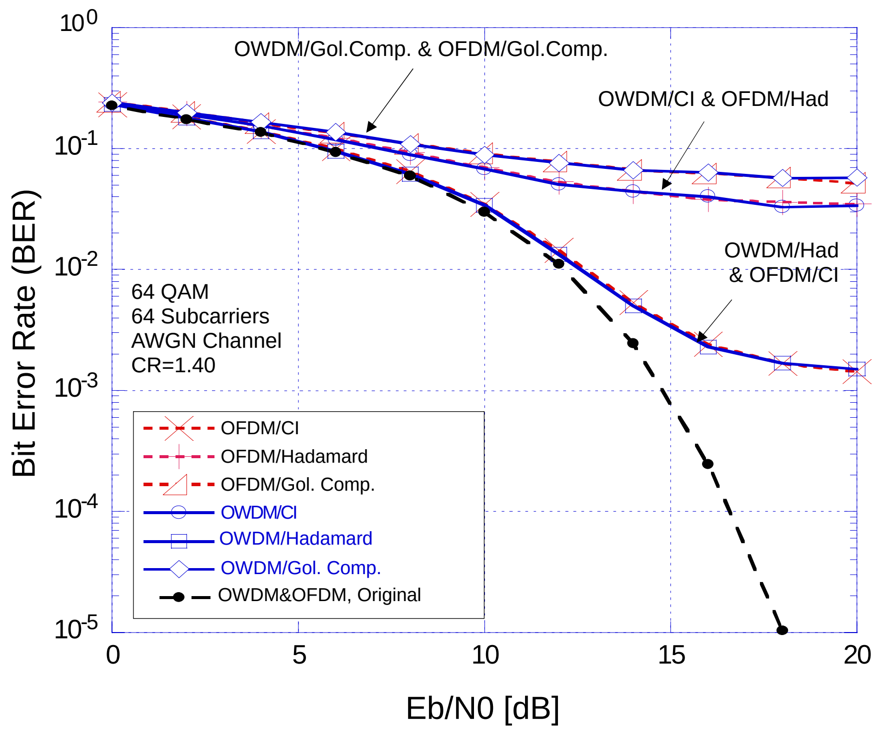

Fig. 2.16 BER Performance of OWDM with Soft Limiter

Fig. 2.16 shows BER performance when CR is 1.40. It is shown that BER with Hadamard is lower even though met floor at BER of $1.5\text{x}10^{-3}$, better than others, which met floor at BER of 4 or $7\text{x}10^{-2}$. Our evaluation with higher CR (over than 1.40) shows that BER curve of Hadamard through all the time is equal to that of the original curve (without clipping).

It is interesting to note that BER performance of OWDM/Hadamard is completely similar to that of OFDM/CI. The same conditions also hold in OWDM/CI & OFDM/Hadamard and OWDM & OFDM with Golay Complementary code. This is due to the perfection similarity properties of PAPR of OWDM and OFDM with any orthogonal spreading codes as explained in the previous section (Fig. 2.10) with load factor of 100%.

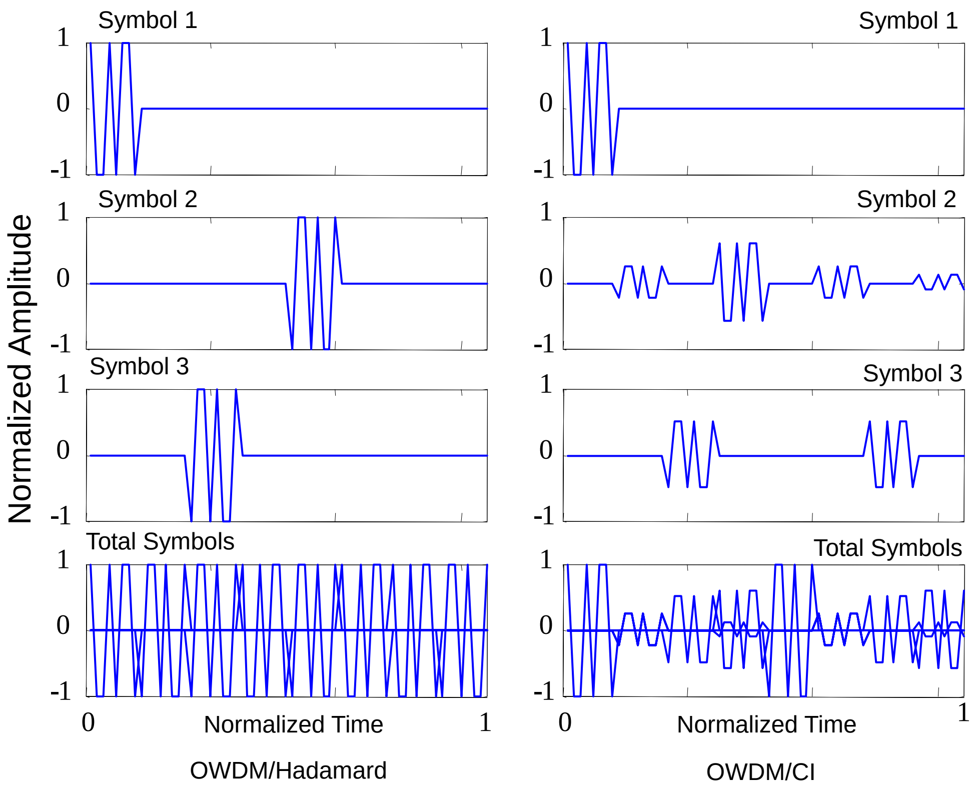

Fig. 2.17 Characteristic of Hadamard and CI on the Envelopes of OWDM Signal

The Secret of Low PAPR

This section discusses how spreading codes reduce the PAPR. We consider Hadamard and CI code due to its good performance in OWDM and OFDM environment. High

PAPR exists yielded by the superposition of a large number of modulated subcarriers in parallel that have same phase (coherently addition). On deep investigating on code performances, low PAPR was then obtained when we can avoid the superposition of signals from each carrier on each transmission which resulted high peaks.

Figs. 2.17 and 2.18 illustrate clearly the envelope of transmitted signals for Hadamard and CI both in OWDM and OFDM environment. Exploration was done by giving an impulse as the input to the system, then we evaluate envelope of the transmitted signal.

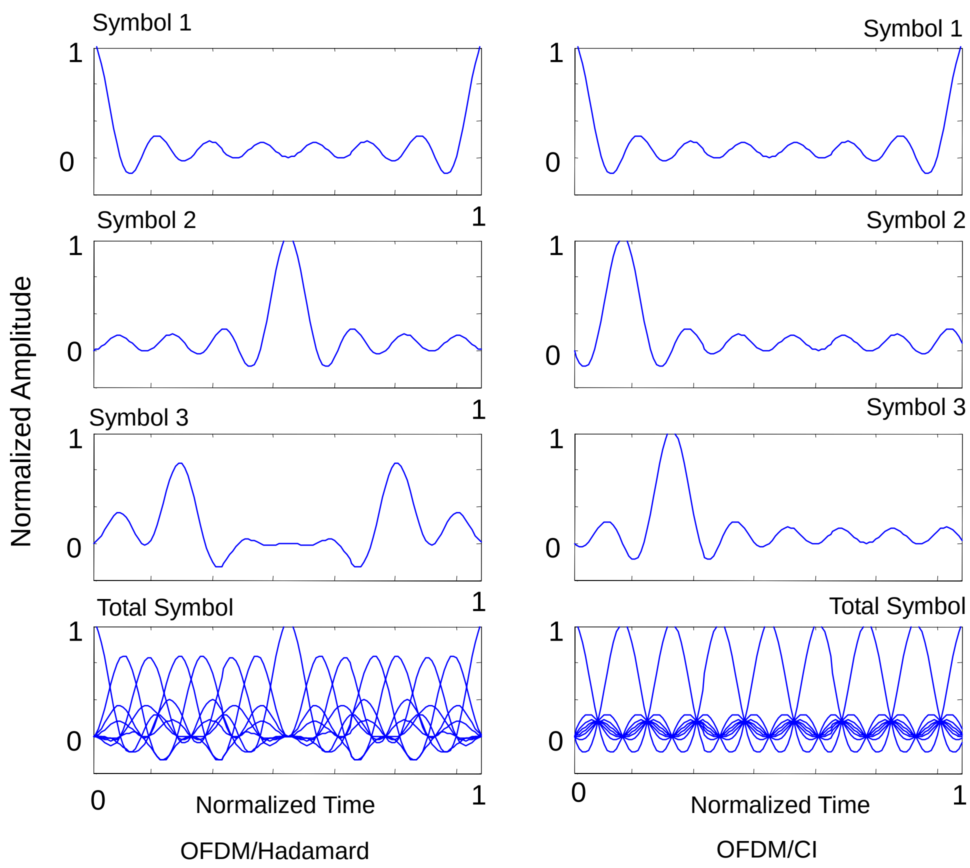

Fig. 2.18 Characteristic of Hadamard and CI Codes on the Envelope of OFDM Signals

Using 8 samples points, we put impulse on the first position e.g. the input for symbol 1= {1 0 0 0 0 0 0 0}, the input for symbol 2 = {0 1 0 0 0 0 0 0}, until input for symbol 8 ={0 0 0 0 0 0 0 1}. By this investigation, we can indicate if any superposition are generated or not, through all of the transmitted signals. The total transmitted signals then illustrate the PAPR properties of the system.

From the Fig. 2.17, envelope of transmitted OWDM signals with Hadamard is flat, similar to that of OFDM signal with CI in Fig. 2.18. The cases of many superposition indications are shown in Fig. 2.17 for OWDM/CI and 2.18 for OFDM/Hadamard.

Chapter 3

Carrier Interferometry OFDM

Recently, there has been some interest in OFDM system using the complex spreading codes, named Carrier Interferometry (CI). CI codes, its derivative which called Pseudo-Orthogonal Carrier Interferometry (PO-CI) codes and their application on OFDM system are evaluated in this chapter. Section 3.1 describes the construction of CI and its envelope fluctuations on BPSK, QPSK, 16QAM and 64QAM OFDM system. This basic investigation is important for PAPR performance analysis of OFDM system. Section 3.2 shows the excellent idea in creating the second set of CI codes by copying from the first set, and how to place it in the "middle" of the previous set, which then results new codes, called PO-CI. In this section the simplification of how to seek the minimum cross correlation between code set 1 and code set 2 is presented.

Section 3.3 evaluates PAPR performance of CI/OFDM and PO-CI/OFDM with data transmission that utilized all and partial subcarriers. Imperfect orthogonality of PO-CI codes is then evaluated with the case of small N and large N, where N is the number of subcarriers. For an easy explanation of the orthogonality of PO-CI codes, the shape of cross correlation matrix and its investigation on the real and imaginer part are also presented. At the last of this section, a number of bit error due to imperfect orthogonality effect of PO-CI codes on BPSK, QPSK, 16QAM and 64QAM is evaluated, followed by analysis of BER performance of OFDM system.

3.1 Carrier Interferometry Codes

Carrier interferometry (CI) is a complex spreading code that is very narrow when is observed in time domain. A CI signal can be easily separated from other CI signals and it is easy to resolve the channel's multipath profiles. Actually this code is the complex phasors of an Inverse Discrete Fourier Transform (IDFT) matrix that is used as a spreading code. This idea is similar to the concept in [9] that used Fast Fourier Transform (FFT) matrix as a spreading code which then results in a single carrier system with a guard interval (GI). However, CI is not a matrix of FFT, so OFDM system that employs CI codes is still a multicarrier system.

Placing in the context of traditional communication signals, the CI signal is a frequency sampled version of the *sinc()* waveform. That is, the CI signal is an approximation to the *sinc()* waveform using N equally spaced samples, where N is the number of carriers. CI codes for k-th symbol is then constructed as

$$CI_k = \{e^{j(2\pi/N)\cdot 0\cdot k}, e^{j(2\pi/N)\cdot 1\cdot k}, e^{j(2\pi/N)\cdot 2\cdot k}, e^{j(2\pi/N)\cdot 3\cdot k}, \cdots, e^{j(2\pi/N)\cdot (N-1)\cdot k}\} \qquad (3.1)$$

The number of these codes is N with length also N, which is usually placed in the matrix with size N x N.

One elegant feature of CI codes is their flexibility. Orthogonal CI codes can be defined for any length N, and are not limited to $N = 2^m$ (i.e. N is a power of two) or $2m$ constraints of the well-known Walsh-Hadamard codes. Other benefit when implemented on OFDM system is its frequency diversity and peak power reduction (evaluation on peak power is presented in detail in the next section). CI codes can be interpreted as masking the multicarrier OFDM system as a single carrier system for PAPR gain, because CI codes employment is able to "cancel" the peak resulted by IFFT and regenerate new fluctuation as single carrier system. In this section, analysis of envelope characteristic of CI on OFDM (CI/OFDM) with some modulations is presented. Detail explanation about how to employ spreading process to OFDM system is in [6], [10-12].

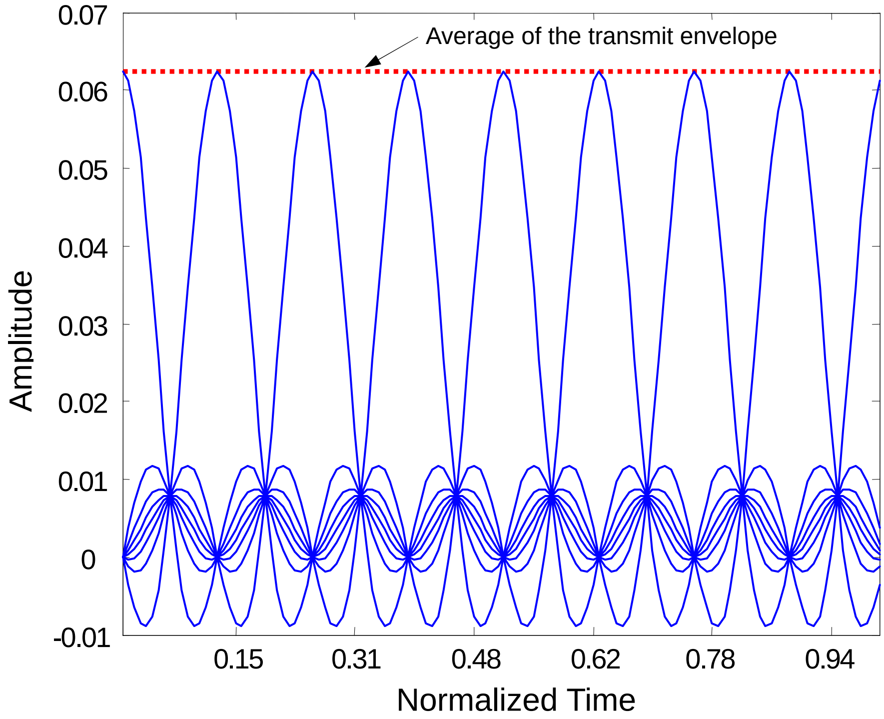

Fig. 3.1 Transmit Envelope of BPSK OFDM with CI Codes

Fig. 3.1 describes the transmit envelope of BPSK OFDM using CI as a spreading code. This figure constructed from BPSK symbol of [1 1 1 1 1 1 1 1] that is spread over all OFDM with 8 subcarriers, and CI codes makes symbols separable at the receiver. It can be seen that when one symbols's subcarrier add coherently, other symbols do not add coherently. It then characterizes the CI/OFDM envelopes are not fluctuated but flat as shown in the summation of the entire signals envelope in Fig. 3.1.

It is important to note that suppose signal at k-th subcarrier ($S_k(t)$) reaches its maximum, the signal at other subcarrier ($S_j(t)$, where $j \neq k$) is at a minimum (i.e. $P_j << P_k$) or a very low value. Hence, constructive combining of all N symbols energy at any one moment in time is not possible, because peak in symbols are evenly spread over OFDM symbol time as illustrated in Fig. 3.1 above. As a result, an excellent PAPR for CI/OFDM symbols is obtained.

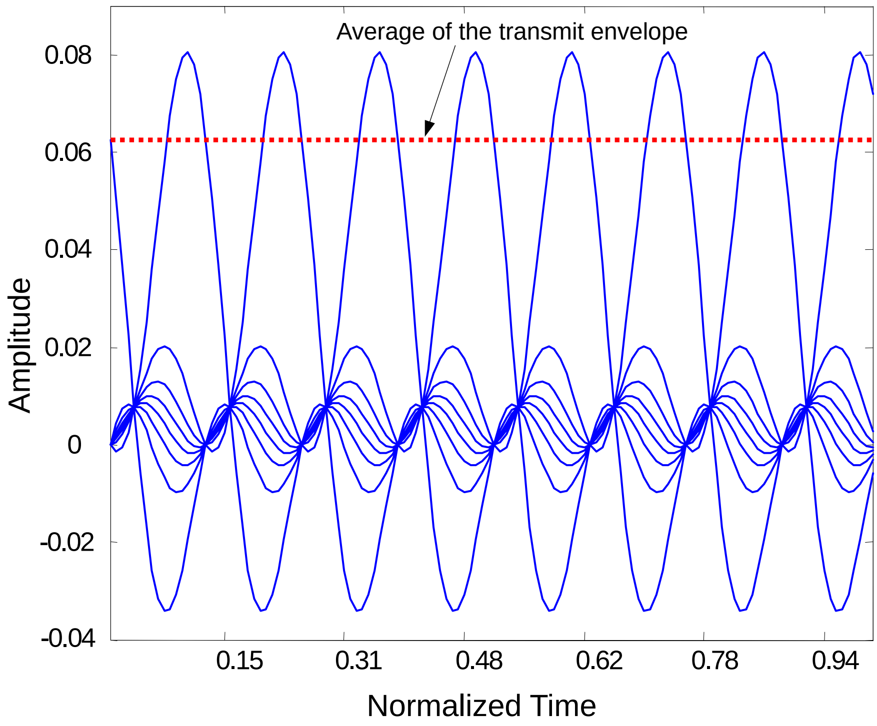

Fig. 3.2 Transmit Envelope of QPSK OFDM with CI Codes

Different modulation impacts to the different characteristic of CI/OFDM envelopes. Fig. 3.2 is plotted from QPSK CI/OFDM with symbols stream is [1+*j*1, 1+*j*1, 1+*j*1, 1+*j*1, 1+*j*1, 1+*j*1, 1+*j*1, 1+*j*1]. However, the waveform is a little different compared to that of with BPSK. QPSK modulation affect to the higher fluctuation of energy per transmitted QPSK symbol, but the total transmitted symbol is similar to BPSK case. This condition makes a special characteristic of the PAPR with BPSK and QPSK are zero dB, because no peak is introduced. From this analysis, it can be concluded that BPSK and QPSK CI/OFDM have a minimum PAPR of zero dB.

It is easy to understand the reason of resulted zero dB. CI can perfectly mask OFDM to single carrier, so BPSK CI/OFDM has peak power of 1^2, and average power also 1. Obviously, we calculate $PAPR_{BPSK\ CI/OFDM} = 10*\log_{10}(1/1) = 0$dB. For the case of QPSK modulation, the maximum peak power is $(-1)^2=1^2$, while the average power is $((1^2 + (-1)^2)/2) = 1$, so the $PAPR_{QPSK\ CI/OFDM} = 10*\log_{10}(1/1) = 0$dB.

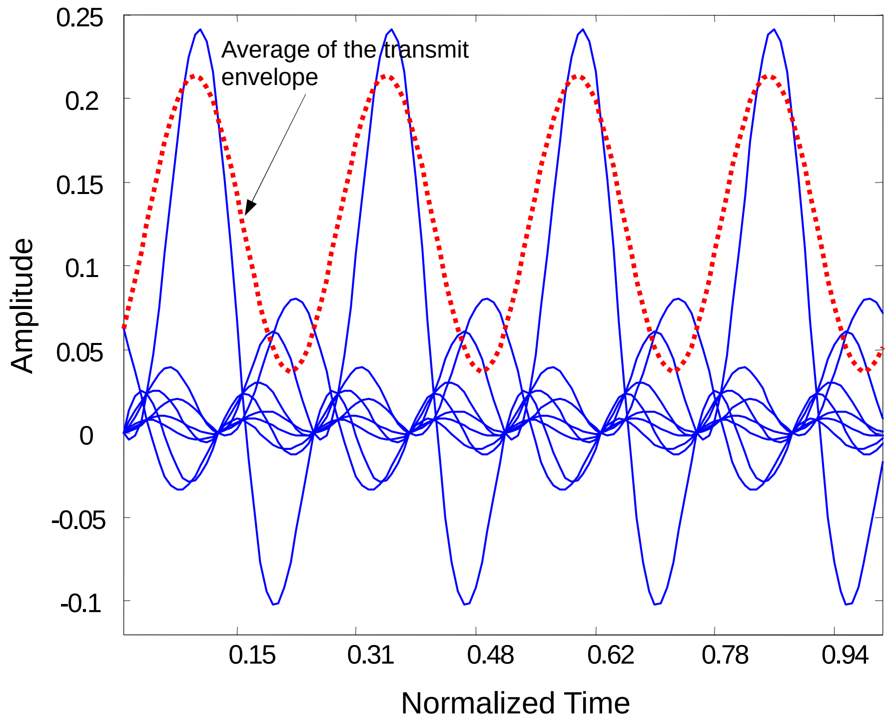

Fig. 3.3 Transmit Envelope 16QAM OFDM with CI Codes

Fig. 3.3 describes the envelope of CI/OFDM with 16QAM modulation. The input symbol stream is [1+*j*1, 3+*j*3, 1+*j*1, 3+*j*3, 1+*j*1, 3+*j*3, 1+*j*1, 3+*j*3] that are inputted to OFDM with 8 subcarriers. Because 16QAM itself is not flat in the amplitude (constructed of combination 1, *j*1, 3 and *j*3), so the output of 16QAM CI/OFDM will not be flat, but returned back to the original fluctuation of 16QAM modulation. Dotted line in Fig. 3.3 is the summation result of all signals from each subcarrier and it shows a sinusoidal rather than a flat signal.

The PAPR is then easy to be calculated. The average power of 16QAM CI/OFDM is $(1^2+3^2)/2 = 5$, with maximum peak power is $3^2 = 9$, so the $PAPR_{16QAM\ CI/OFDM} = 10*\log_{10}(9/5) = 10*\log_{10}(1.80) = 2.5527$dB. The computer calculation also confirmed the same value on CDF of 99.99%.

Fig. 3.4 illustrates 64QAM CI/OFDM signal envelope with input of symbol stream is [1+*j*1, 3+*j*3, 5+*j*5, 7+*j*7, 1+*j*1, 3+*j*3, 5+*j*5, 7+*j*7]. The envelope fluctuation in this signal is also not flat and more dynamics in compared with the case of 16QAM. This condition leads to the higher PAPR level than that of in 16QAM. This PAPR can be derived from the 64QAM constellation. Average power is $(1^2+3^2+5^2+7^2)/4 = 21$. Then maximum instantaneous peak power is $7^2 = 49$. The PAPR is then calculated as $PAPR_{64QAM\ CI/OFDM} = 10*\log_{10}(49/21) = 3.678$dB. This value also has been confirmed by computer simulation on CDF of 99.99% and presented in Fig. 3.8 of section 3.3.1.

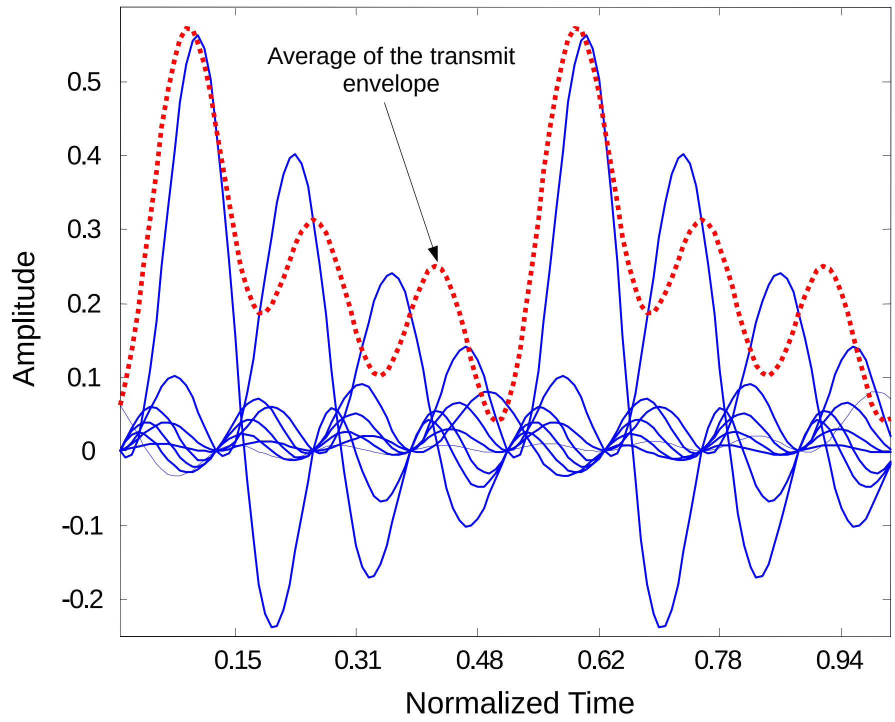

Fig. 3.4 Transmit Envelope of 64QAM OFDM with CI Codes

3.2. Pseudo-Orthogonal Carrier Interferometry Codes

Pseudo-Orthogonal Carrier Interferometry (PO-CI) spreading codes have been introduced to increase the throughput and also the performance of OFDM and MC-CDMA system [6] and [10-12]. With these codes, it is reported that the OFDM and MC-CDMA throughput are capable to be doubled, because 2*N* parallel data streams can be coded onto N subcarriers. Then, it is stated that high throughput and high performance OFDM and MC-CDMA can be achieved by utilizing PO-CI codes. However, there will be a limitation of PO-CI codes due to its un-orthogonality properties. The main contribution of this section is then performing the analysis of the PO-CI codes orthogonality and verified its performance on OFDM with M-QAM modulations.

PO-CI codes contain two sets of CI codes in order enables of increasing the throughput doubled. The second code set is the copy of the first set. Illustration about these sets with N=8 is presented in Fig. 3.5. CI codes in set 1 are orthogonal to one another and CI codes in set 2 are also orthogonal to one another. However, the CI codes in set 1 are not orthogonal to the CI codes in set 2. This problem is then solved by seeking $\Delta\theta$ that is able to minimize the cross correlation between these codes sets.

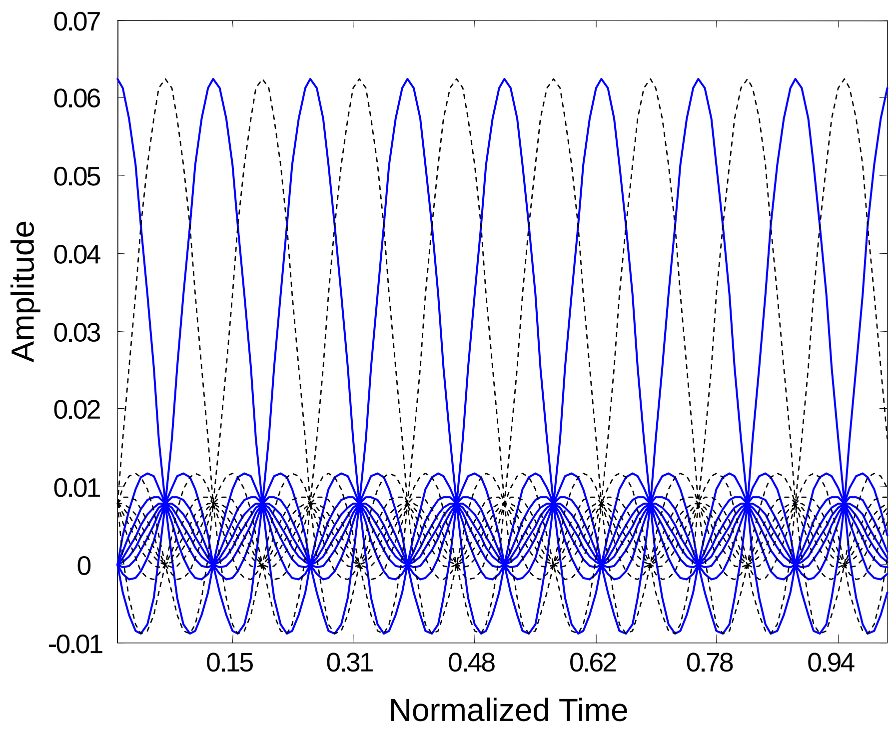

Fig. 3.5 Transmit Envelope of BPSK OFDM with PO-CI Codes

(code set 1: solid line, code set 2: dotted line)

Codes set 1 of PO-CI are the CI code as expressed in (3.1) and rewritten as

$$C1_k = \left\{ e^{j(2\pi/N)\cdot 0\cdot k}, e^{j(2\pi/N)\cdot 1\cdot k}, e^{j(2\pi/N)\cdot 2\cdot k}, \cdots, e^{j(2\pi/N)\cdot (N-1)\cdot k} \right\} \tag{3.2}$$

and the codes set 2 for k=N, N+1, …, 2N-1, is expressed as

$$C2_k = \left\{ e^{j\{(2\pi/N)0\cdot k+0\cdot\Delta\theta\}}, e^{j\{(2\pi/N)1\cdot k+1\cdot\Delta\theta\}}, e^{j\{(2\pi/N)2\cdot k+2\cdot\Delta\theta\}}, \cdots, e^{j\{(2\pi/N)(N-1)\cdot k+(N-1)\cdot\Delta\theta\}} \right\} \tag{3.3}$$

For obtaining orthogonal or pseudo-orthogonal codes, $\Delta\theta$ must be selected to minimize the cross correlation between code set 1 and code set 2. Let $R_{1,2}(m,n)$ refer to the cross correlation between the m-th spreading sequence in orthogonal code set 1 (3.2) and n-th spreading sequence in orthogonal code set 2 (3.3). Also let

$$R_{1,2} = \left[\frac{1}{N^2} \sum_{m=0}^{N-1} \sum_{n=0}^{N-1} \left(R_{1,2}(m,n) \right)^2 \right]^{1/2} \tag{3.4}$$

represent the root mean square (*rms*) cross correlation that exist between spreading sequence in code set 1 and set 2. Now, it is easy to show that for real signalling

$$\begin{aligned} R_{1,2}(m,n) &= \frac{1}{2\Delta f} \sum_{k=0}^{N-1} \cos\left[k(\theta_m - (\theta_n + \Delta\theta)) \right] \\ &= \frac{1}{2\Delta f} \sum_{k=0}^{N-1} \cos\left[k\left(\frac{2\pi}{N} m - \frac{2\pi}{N} n - \Delta\theta \right) \right] \end{aligned} \tag{3.5}$$

It is also easy to show that

$$\sum_{k=0}^{N-1} \left(R_{1,2}(m,n) \right)^2 = \sum_{k=0}^{N-1} \left(R_{1,2'}(m,n') \right)^2, k \neq k' \tag{3.6}$$

That is the total cross correlation between the n-th spreading code in orthogonal code set 2 and all spreading sequence in group 1. Using (3.6), equation (3.4) can be rewritten as

$$R_{1,2} = \left[\frac{1}{N} \sum_{m=0}^{N-1} \left(R_{1,2}(m,0) \right)^2 \right]^{1/2} \tag{3.7}$$

and using (3.5), this become

$$R_{1,2} = \left[\frac{1}{N} \sum_{m=0}^{N-1} \left[\frac{1}{2\Delta f} \sum_{k=0}^{N-1} \cos\left[k(\frac{2\pi}{N} m - \Delta\theta) \right] \right]^2 \right]^{1/2} \tag{3.8}$$

Let us now determine the selection of $\Delta\theta$ for code set 2 that minimize the *rms* cross correlation between the two orthogonal code sets. To do this, we select

$$\frac{\partial R_{1,2}}{\partial \Delta\theta} = 0 \tag{3.9}$$

Now,

$$\begin{aligned} \frac{\partial R_{1,2}}{\partial \Delta\theta} &= \frac{1}{2} \left[\frac{1}{N} \sum_{m=0}^{N-1} \left(R_{1,2}(m,0) \right)^2 \right]^{-(1/2)} \cdot \frac{1}{N} \frac{\partial \left[\sum_{m=0}^{N-1} \left(R_{1,2}(m,0) \right)^2 \right]}{\partial \Delta\theta} \\ &= \frac{1}{2} \left[\frac{1}{N} \sum_{m=0}^{N-1} (R_{1,2}(m,0))^2 \right]^{-(1/2)} \cdot \frac{1}{N} I \end{aligned} \tag{3.10}$$

where

$$\begin{aligned} I &= \frac{\partial \left[\sum_{m=0}^{N-1} (R_{1,2}(m,0))^2 \right]}{\partial \Delta\theta} \\ &= \frac{\partial \left[\sum_{m=0}^{N-1} \left(\sum_{k=0}^{N-1} \cos\left[k\left(\frac{2\pi}{N} m - \Delta\theta \right) \right] \right)^2 \right]}{\partial \Delta\theta} \end{aligned} \tag{3.11}$$

when $\Delta\theta = k\pi/N, k = 0,1,2...$, we have I=0 and therefore (3.10), $\partial R_{1,2}/\partial\Delta\theta = 0$. Seeking to determine which $\Delta\theta$ are maxima and which are minima, we calculate the second order partial derivative at $\Delta\theta = k\pi/N$ and determine

$$\frac{\partial R^2}{\partial^2 \Delta\theta} > 0 \quad \text{when} \quad \Delta\theta = \frac{(2k+1)\pi}{N} \quad \text{(minima)} \tag{3.12}$$

$$\frac{\partial R^2}{\partial^2 \Delta\theta} < 0 \quad \text{when} \quad \Delta\theta = \frac{2k\pi}{N} \quad \text{(maxima)} \tag{3.13}$$

The derivation explained above is the explanation for obtaining PO-CI code in [6] and we correct some ambiguous symbol. Hence, cross correlation is minimum when setting $\Delta\theta = (2k+1)\pi/N$, for simplicity we can select k=0 and obtain $\Delta\theta = \pi/N$ for the minimum cross correlation, i.e., $R_{1,2} = 1/\sqrt{N}$. It is believed in [6] and [11], that when N is large the *rms* cross correlation is low and the code becomes an excellent code.

However, our results clarify that PO-CI codes work only with the BPSK modulation and not longer efficient for M-QAM modulation (QPSK, 16QAM or 64QAM) due to its imperfect orthogonality, mainly on the imaginary parts even N is large.

3.3. Evaluations

This evaluation is presented for PAPR performance of CI/OFDM when only partial subcarriers are utilized for data transmission, and imperfect orthogonality analysis of PO-CI codes on M-QAM OFDM System. BER performance with PO-CI codes is then performed with BPSK, QPSK, 16QAM and 64QAM at the last section of this chapter.

3.3.1 PAPR Performance Evaluation

Practically, not all subcarriers are used for data transmissions but some of them are for pilot or zeroed for the reason of reducing the adjacent inter-carrier interference. IEEE.802.11a using only 48 subcarrier from 64 generated subcarriers, 4 of them are for pilot and other 12 subcarriers are zeroed. BER for data transmission using all subcarriers should be compared to that of using only some parts of the subcarrier. For this reason, numerical result with computer simulation is plotted in Fig. 3.6.

Fig. 3.6 is generated from QPSK modulation with 128 subcarriers and 32 are zeroed. It means that only 96 subcarriers are used for data transmissions. This figure shows that using partial subcarriers is better for the reason of reducing inter-carrier interference which results in the improvement on the BER performance (2 dB better for all E_b/N_0 level). This result is correct because with the zeroed subcarriers the inter-carrier interference is able to be reduced.

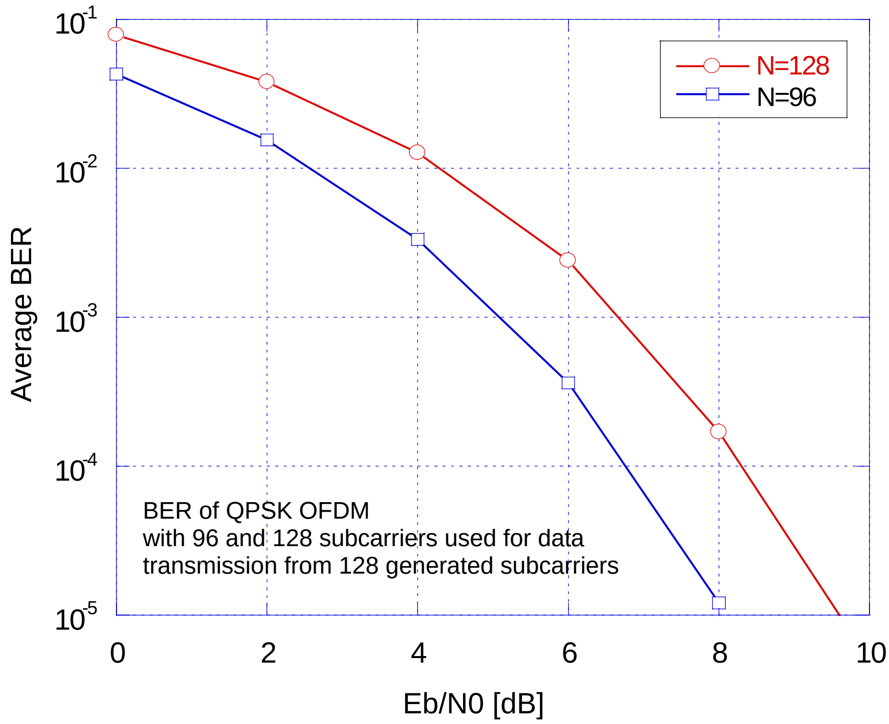

Fig. 3.6 The Improvement of BER Performance by Using Partial Subcarrier for Data Transmissions

As explained in section 3.1, CI ensures that when one symbol's carrier adds coherently other symbol's carrier do not add coherently, and resulted in OFDM symbol with stable envelop as in Fig. 3.1 and 3.2. However, the use of partial subcarriers affects the performance degradation of CI code in composing stable envelope [13].

In this section, we evaluated PAPR performance both in case that full subcarriers and parts of subcarriers are used. In case that some carrier is zeroed, CI could not work perfectly in avoiding superposition of symbols and it impacts to the peak appearances on the transmitted OFDM symbols as illustrated in Fig. 3.7. The PAPR then confirmed increases as the increasing in subcarriers number. This condition is exactly contrasts to the PAPR performance when all subcarriers are utilized for data transmission.

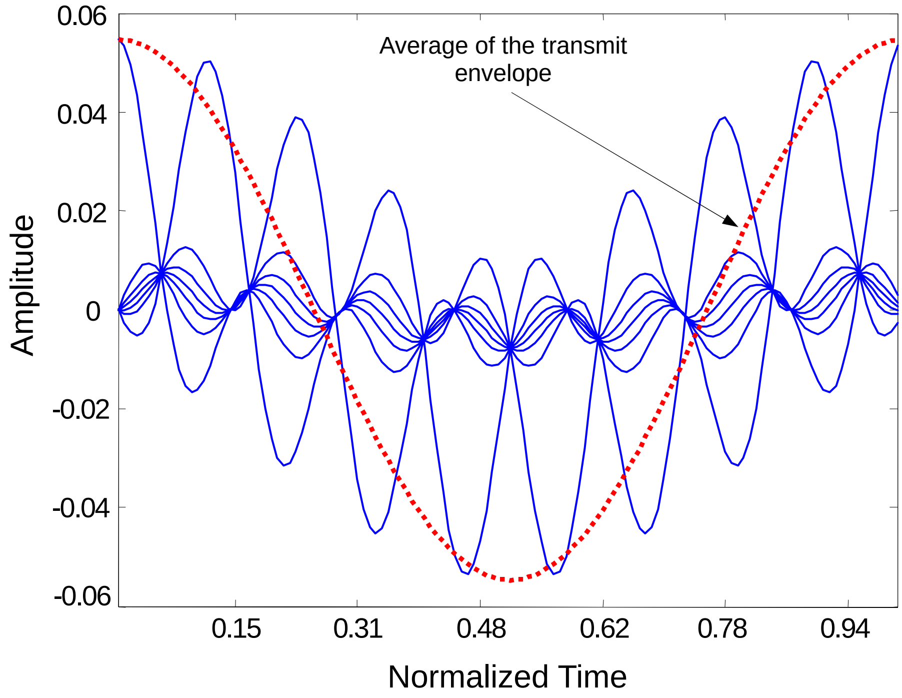

Fig. 3.7 Effect of Partial Subcarrier to the Fluctuations of CI Transmit Envelope

Fig. 3.7 illustrates the dynamic fluctuation of envelope when only partial subcarrier is used. This figure is generated from BPSK CI/OFDM where frequency zero (DC part) is not used, so the input is only [1 1 1   1 1 1 1]. This graph is significantly dissimilar to the Fig. 3.1 even only one subcarrier is not used. Hence, the PAPR will increase from zero dB to approximately 9dB at CDF of 99.99%. It means CI codes is only able to reduce the PAPR of OFDM approximately 2dB, from 12dB reduced up to 9dB when minimally one subcarrier is zeroed.

Through all this section, we consider partial subcarrier utilization as specified by IEEE.802.11a Standard, which 75% of subcarrier is utilized for data transmissions. We put zero on the left and right side of the subcarriers and frequency zero is not used. It is clearly illustrated as

$$\{0\ 0\ 0\ 0\ 0\ 0,\ f_{-24},\ \ldots,\ f_{-1},\ 0,\ f_1,\ldots,\ f_{24},\ 0\ 0\ 0\ 0\ 0\},$$

and without loss of generality, we can put zero in the middle of the subcarriers or we may ignore the pilot. The lengths of CI codes are then created as the number of this “active” subcarriers. We then adopt this configuration scheme for other large number of evaluations i.e. 128, 256, 512, and 1024 FFT points with 25% of subcarrier are zeroed. This condition is possible with CI codes, because CI codes are flexible to the number of subcarriers even it is not power of two.

Further PAPR calculations with 64QAM are plotted in Fig. 3.8 and 3.9, for making sure how deep partial subcarrier utilization affects to the PAPR performance. It is then confirmed that an excellent PAPR reduction is achieved when all subcarriers are utilized, while PAPR are still high when only some part of subcarrier utilized for data transmission.

It is interesting to note that in case of using all subcarrier as data transmissions; the PAPR will decrease when we increase the subcarriers number as shown in Fig. 3.8. PAPR of subcarrier 1024 is 3.7dB, less then that of 64 with PAPR value of 5dB. The reason is CI works more perfectly on large number of subcarriers.

As concluded in Fig. 3.8 and analysis of Fig. 3.4, by the increasing number of subcarrier, the PAPR will meet the theoretical PAPR that was calculated for 64QAM i.e. 3.67dB. This is the lower bound of PAPR 64QAM CI/OFDM. Fig. 3.9 describes PAPR performance with partial subcarriers utilization.

When only partial subcarriers are utilized, this condition is precisely contrast to the condition of utilizing all subcarriers. Even though the PAPR is lower compared to the original OFDM, PAPR increases as the increasing in subcarriers number as illustrated in Fig. 3.9. PAPR with subcarrier 64 is by about 8.5dB, less then that of with 1024 subcarriers with PAPR level of 9.5dB. This condition requires other PAPR reduction technique which is capable of reducing the remaining PAPR significantly. We propose new efficient method that presented in chapter 5 and 6.

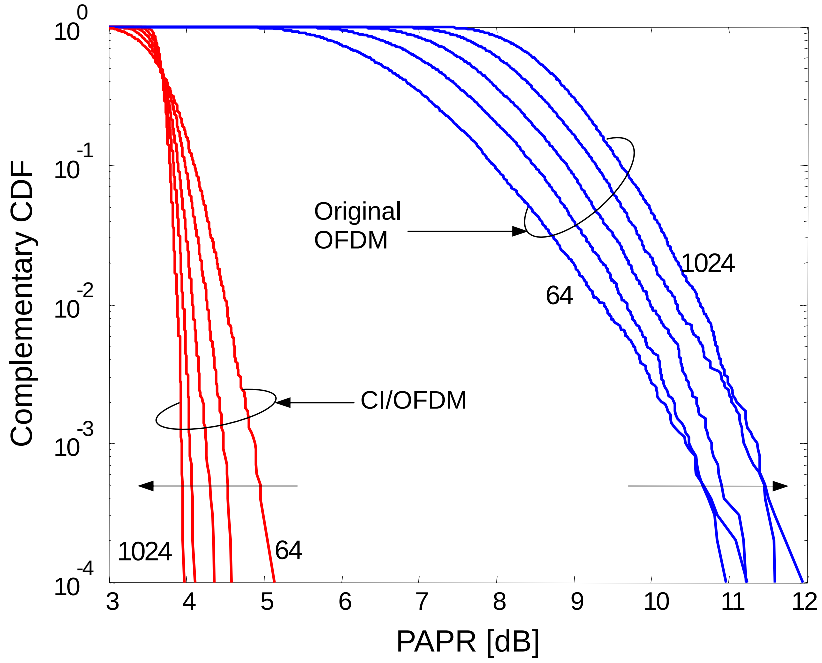

Fig. 3.8 OFDM PAPR Performance with CI Code when All Subcarrier are Dedicated for Data Transmissions

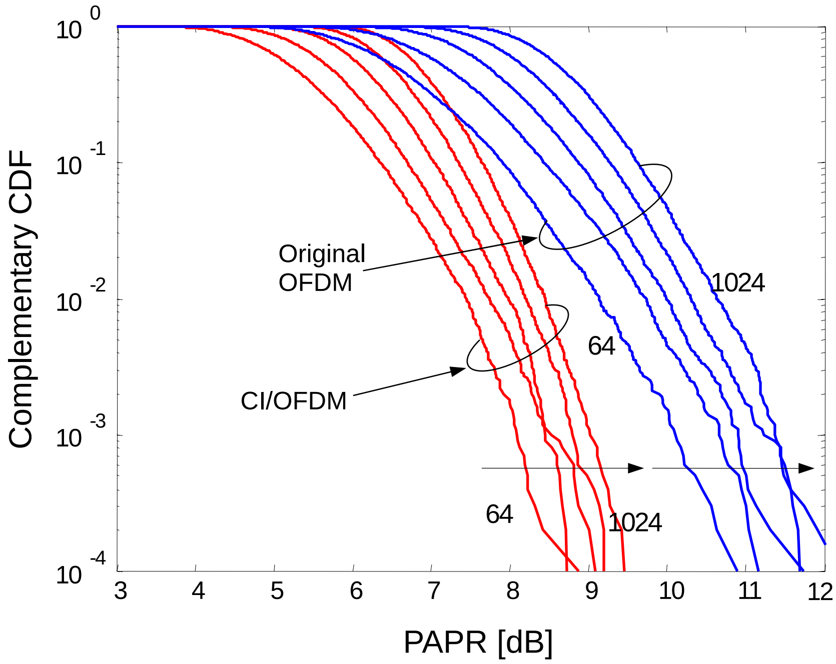

Fig. 3.9 OFDM PAPR Performance with CI Code when Only Partial Subcarrier are Dedicated for Data Transmissions

Fig. 3.9 clearly evaluated PAPR performance of CI/OFDM in case on only partial subcarriers are dedicated for data transmissions. Now, our evaluation can be extended to PO-CI codes. These codes have different characteristic compared to CI codes performance in reducing the PAPR.

PO-CI codes performance on reducing PAPR of BPSK PO-CI/OFDM is plotted in Fig. 3.10. FFT point is 128, while zeroed subcarriers are 32 subcarriers. When all subcarriers are dedicated for data transmission, PAPR with PO-CI codes is not zero dB as analyzed in Fig. 3.1 and 3.2. It means that envelope with PO-CI codes is not flat. This envelope then affect to the PAPR of PO-CI/OFDM 6.5dB on CDF of 99.99%.

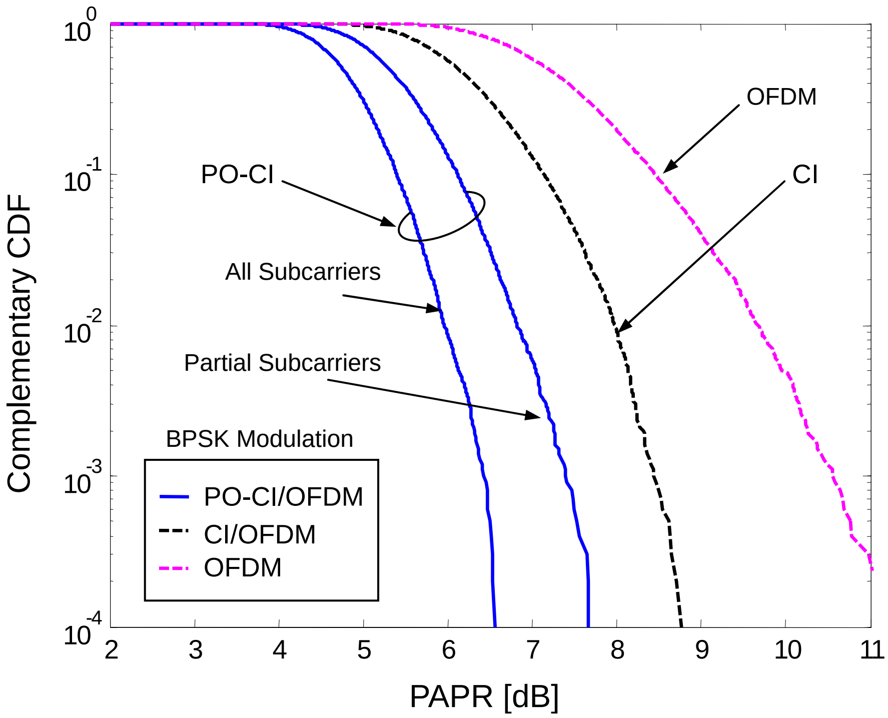

Fig. 3.10 OFDM PAPR Performance with PO-CI Code when All and Partial Subcarriers are Dedicated for Data Transmission

When only partial subcarriers are utilized for data transmission, PAPR with PO-CI codes increased 1dB, up to approximately 7.5dB. It is interesting to note that this PAPR is lower compared to the CI/OFDM with PAPR is about 8.7dB. It means that PO-CI codes have other benefit compared to CI codes. The first benefit is OFDM throughput can be doubled and secondly, PAPR is lower compared to CI codes in case of partial subcarriers for data transmissions.

We conclude generally that PAPR of CI/OFDM is still high and need to be reduced more lowly. Though, PO-CI codes have PAPR characteristic lower than CI codes, but the reduction using PO-CI is only 1dB. Other demerit is that PO-CI codes don't have good orthogonality property. This conclusion then leads us to seek other PAPR reduction method that is capable of reducing the PAPR significantly with minimum performance degradation.

We propose an efficient PAPR reduction technique for OFDM system called CI/IP (Carrier Interferometry/Iterative Processing) technique [14], which will be presented in the next chapter. This technique is capable of reducing the PAPR significantly. The proposed technique uses iterative processing for clipping the high peak to obtain the desired threshold level. The difference from normal OFDM clipping is the effect of spectrum broadening and the BER performance degradation. CI/IP does not introduce spectrum broadening while minimizing the BER performance degradation, but as the payment for this, CI/IP requires the increasing of the calculation amount by iteratively clipping the high peak over the threshold level.

3.3.2 Imperfect Orthogonality of PO-CI Codes

In this section, the analysis of imperfect orthogonality PO-CI codes is presented. With these codes, it is reported that the OFDM and MC-CDMA throughput are capable to be doubled, because $2N$ parallel data streams can be coded onto N subcarriers. Then, it is claimed that high throughput and high performance OFDM and MC-CDMA can be achieved by utilizing PO-CI codes. However, we found some limitation of PO-CI codes related to its un-orthogonality properties [14].

The main contribution of this subsection is performing the analysis of the PO-CI codes orthogonality and verified its performance on OFDM system with *M*-QAM modulations. Our results clarify that PO-CI codes work only with the BPSK modulation and not longer efficient for *M*-QAM modulation (QPSK, 16QAM or 64QAM) due to its imperfect orthogonality, mainly on the imaginary parts.

How to construct these PO-CI codes has been clearly explained in section 3.2 and will not repeated in this section. These codes have length twice of the CI length as a consequence of the capability to increase the throughput doubled. However, our deep investigation on these codes found some limitation that affects the code flexibility when combining to the modulation such as QPSK, 16QAM and 64QAM. First, we check the cross correlation properties with small and large N, where N is the number of OFDM subcarriers and also the number of the codes. Secondly, we observed the constellation of symbol after transmitted using these PO-CI codes and calculating the number of bit errors. Finally we perform the investigation on PO-CI/OFDM with BPSK, QPSK, 16QAM and 64QAM modulation.

Papers [16][17] proved mathematically that when $\Delta\theta = \pi/N$, the cross correlation $R_{1,2}$ between the sets is minimum with cross correlation value of $R_{1,2}=1/\sqrt{N}$. The mathematical derivation for this $R_{1,2}$ has been explained in section 3.2 of this chapter. Figs. 3.11 and 3.12 compare the shape of cross correlation matrix (see Appendix) of CI codes, which have perfect orthogonality, and PO-CI code, which have pseudo-orthogonality. However, the shape of cross correlation shows that the cross correlation matrix is not too small for guaranteeing no interferences between codes (inter-code interference). The un-orthogonality parts still remained even the number N of subcarrier is increased from N=8 to N=512. This condition makes BER performance of PO-CI codes can not be improved even N is high (except for BPSK) and it is contrast to the expectation of [16] that PO-CI codes will be an excellent codes if N is high. In fact, these codes are required to be re-evaluated and re-structured in order to have good and improved orthogonality properties, so it is applicable to many modulation schemes.

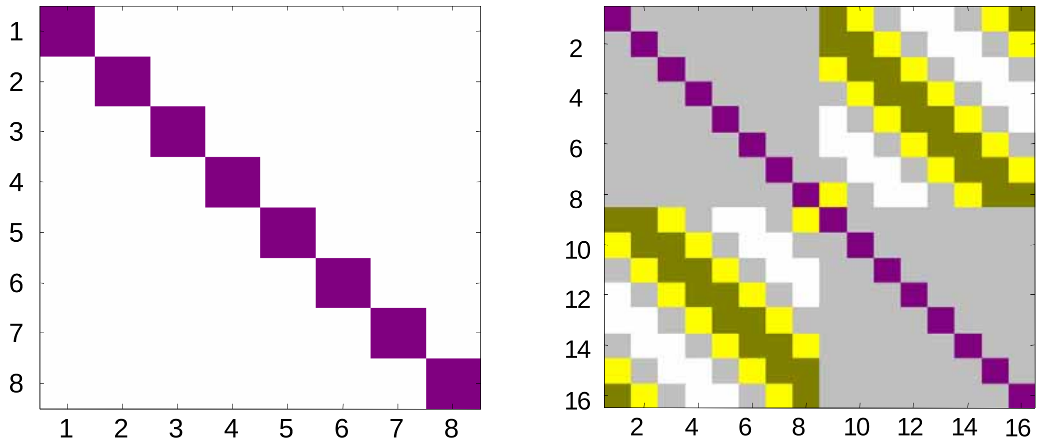

(a). CI (8 codes with length of 8) (b). PO-CI (8 codes with length of 16)

Fig. 3.11 Shape of the Cross Correlation Matrix with Small *N* (*N*=8).

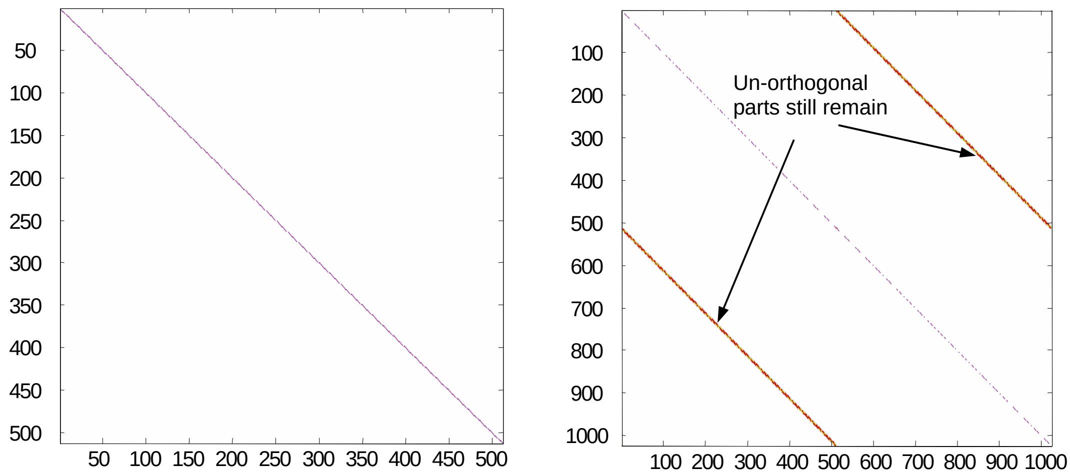

(c). CI (512 codes with length of 512) (d). PO-CI (512 codes with length of 1024)

Fig. 3.12 Shape of Cross Correlation Matrix with large *N* (*N*=512)

The most un-orthogonality of PO-CI codes, even *N* is large, is caused by the imaginary part of these codes. Fig. 3.13(c) and (d) confirm this condition. It is then concluded that remaining un-orthogonality of PO-CI codes in Fig. 3.12(b) and (d) is due to this imaginary part which is the most un-orthogonal part. In Fig. 3.13, it is confirmed that the imaginary part should be zero for obtaining a perfect orthogonality.

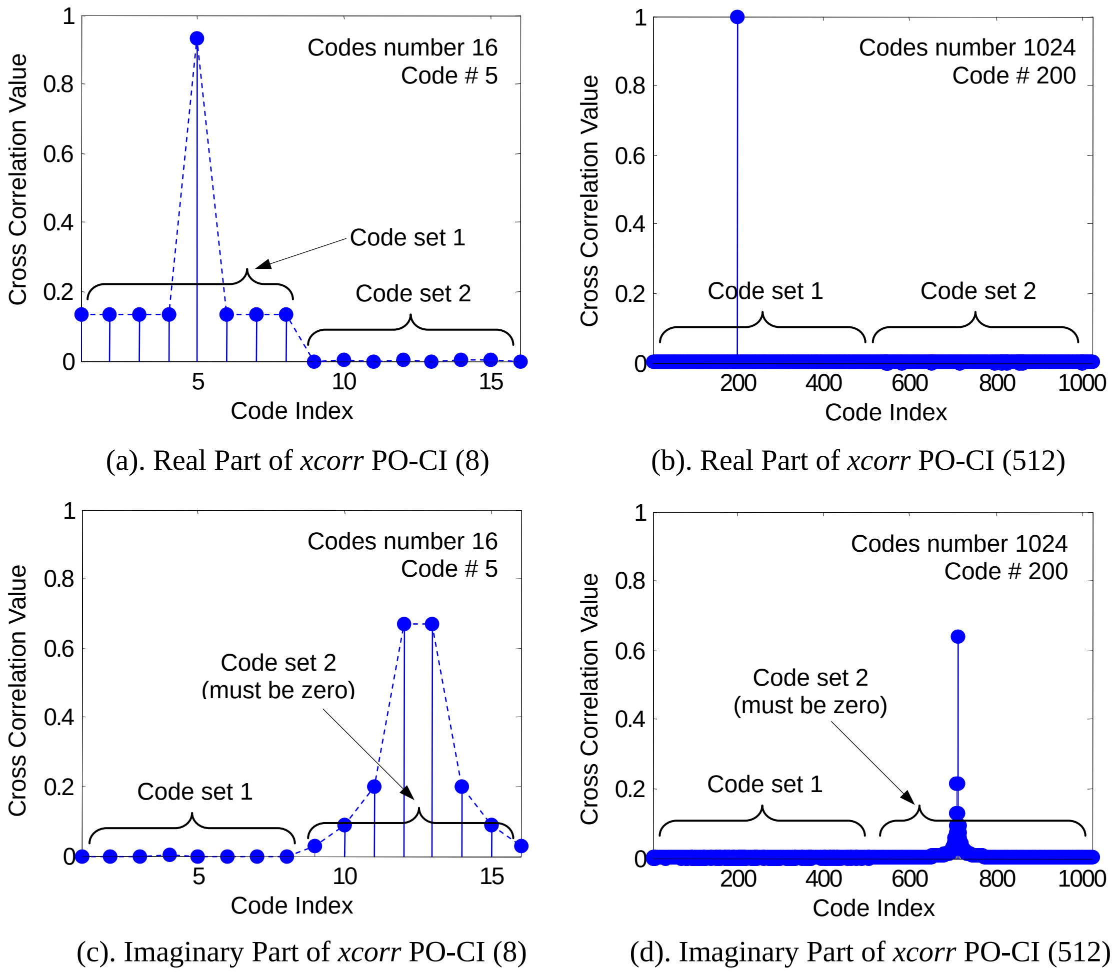

Fig. 3.13 Real and Imaginary Part of Cross Correlation PO-CI Codes for N=8 and N=512 (*xcorr* = cross correlation)

Fig. 3.13 shows the cross correlation between code#5 of POCI with N=8, and code#200 of PO-CI with N=512. The real part is good, when N is large, but the imaginary part still remains cross correlation that is not zero. This remaining cross correlation should be reduced by re-structuring the construction of PO-CI codes especially the second sets. Un-orthogonality in imaginary part as shown in Fig. 3.13 (c) and (d) is the reason why PO-CI is only applicable to BPSK but not for higher order modulation that has imaginary part i.e. M-QAM modulation.

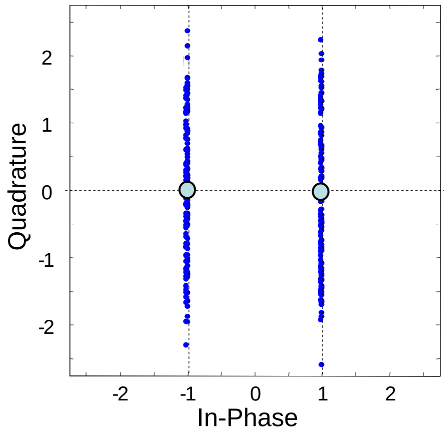

(a). BPSK

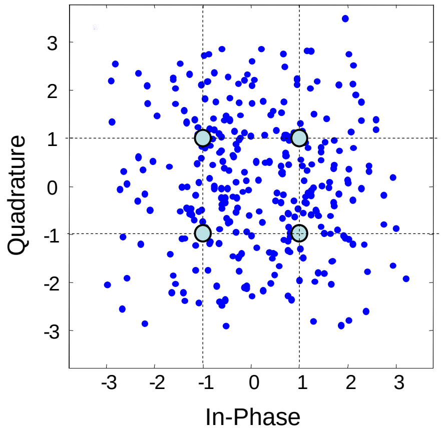

(b). QPSK

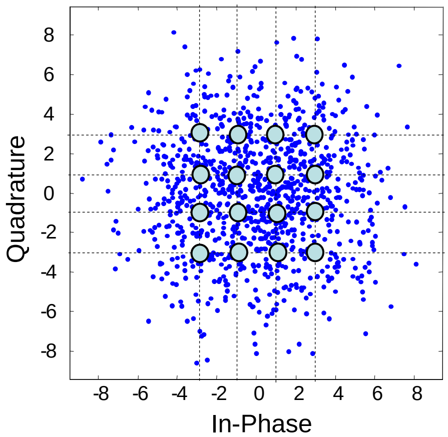

(c). 16QAM

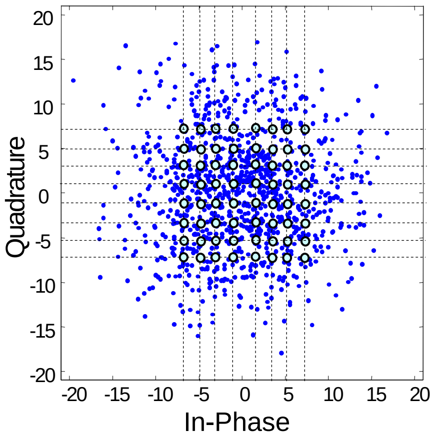

(d). 64QAM

Fig. 3.14 Constellation of BPSK, QPSK, 16QAM and 64QAM with PO-CI Code

Fig. 3.14 shows the BPSK, QPSK, 16QAM and 64QAM constellation after PO-CI codes are utilized. For BPSK, it may be good enough, even the remaining imaginary part is still appears. However, *M*-QAM modulation as presented in Fig. 3.14 (b), (c) and (d) are destroyed by PO-CI codes and impossible to be perfectly recovered at the receiver. Many *M*-QAM symbols are error due to imperfect orthogonality of PO-CI codes. This fact confirms the result of Figs. 3.13 and 3.14 that the real part is good enough, so it is possible for BPSK modulation to be transmitted using PO-CI codes, but the cross correlation of the imaginary part is not enough for keeping the symbol without interference from the others, and it impacts on the constellation destruction of M-QAM modulation which have imaginary part.

Our computer simulation results in Fig. 3.15 then confirm numerically, how deep the error arises on each of the modulations schemes. This result was plotted from 1000 symbols which are transmitted using PO-CI codes. With BPSK, the error is approximately zero when N is large, but the error is not zero when N<16. The error of QPSK is approximately 17%, 16QAM is 30% and 64QAM is 39%. It is clearly shown that PO-CI codes are not longer efficient for M-QAM modulation due to big errors which could not be neglected. Further improvement of PO-CI codes should be started from improving the imaginary part of PO-CI codes.

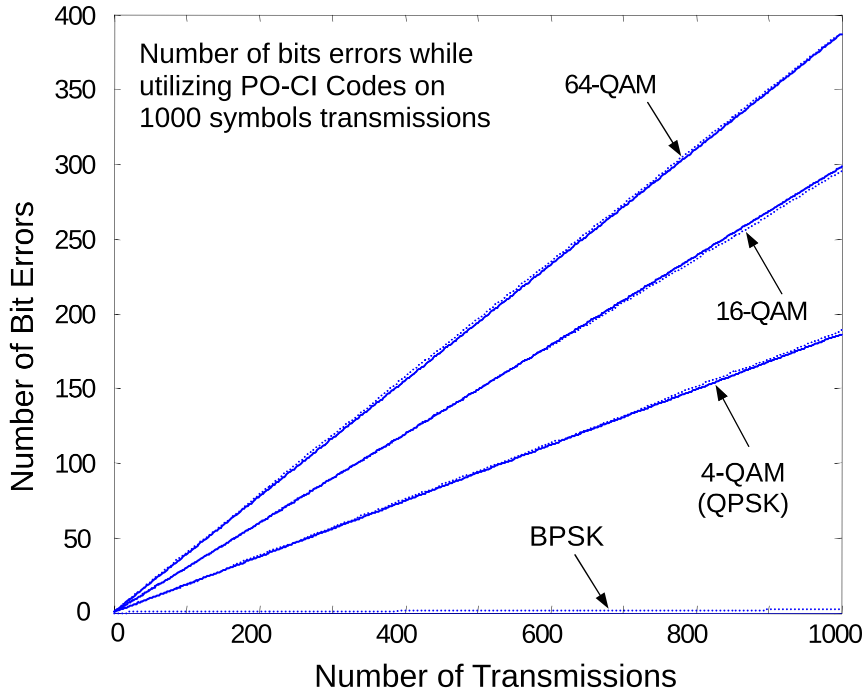

Fig. 3.15 Number of Bits Error on BPSK, QPSK, 16QAM and 64QAM when were Transmitted Using PO-CI Code

Fig. 3.16 shows the BER performance of PO-CI/OFDM with BPSK modulation. With *N* equal to 8, PO-CI codes influence error floor at BER of $3\text{x}10^{-3}$. When *N* is increased to be *N*=512, BER performance is improved to be similar to the BER performance of 16QAM, which has 3dB degradation compared to the original BER of BPSK ideal for all E_b/N_0.

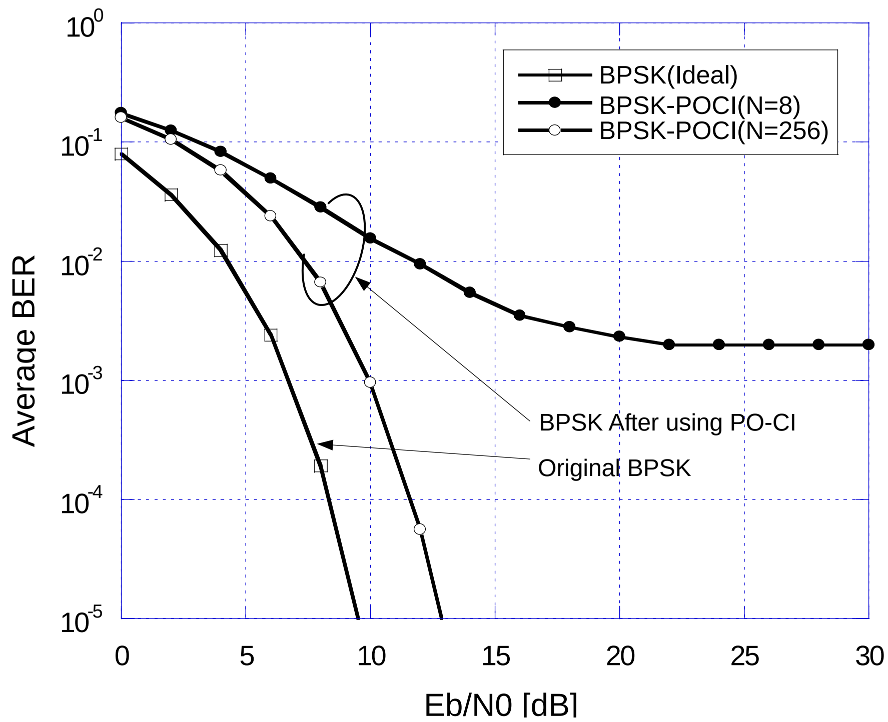

Fig. 3.16 BER Performance BPSK OFDM with PO-CI Codes

Fig. 3.17 presents BER performance of PO-CI/OFDM with M-QAM modulations. BER performance with *M*-QAM (QPSK, 16QAM and 64QAM) shows error floor on BER of $2\text{-}3\text{x}10^{-1}$ and it is not improved even when *N* is large (*N*=128).

PO-CI codes work only for BPSK with large *N*, because the orthogonality of real part is good when *N* is large. Unfortunately, the imaginary part is not improved even when *N* is large. It is the fact that supports the result as shown Figs. 3.13, 3.14 and 3.15. Papers in [6] and [10]-[12] also only use BPSK as the modulation scheme.

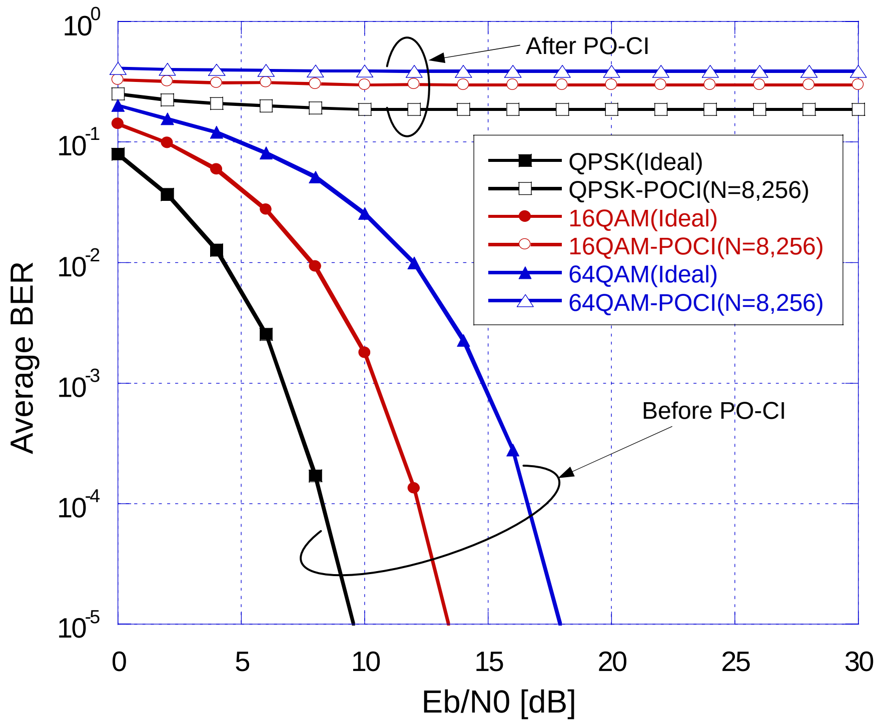

Fig. 3.17 BER Performance of *M*-QAM OFDM with PO-CI Codes

Figs. 3.15, 3.16 and 3.17 lead us to improve the performance of PO-CI codes. There are two ways of how to improve it. The first way is re-constructing the structure of the codes that result in codes with better orthogonality properties e.g. smaller (or zero) value of cross correlation in imaginary part compared to Fig. 3.13. The second way is by introducing inter-code interference canceller. It is possible because there is a good pattern of un-orthogonality inside the PO-CI codes constellation.

Chapter 4

Iterative Processing Method

In section 2.3 we have discussed PAPR reduction method. An example of PAPR reduction with distortion is a clipping. Clipping is the easiest technique for the peak reduction. However, it introduces large BER degradation and out-of-band noise.

Iterative processing (IP) is one kind of PAPR reduction method that allowed distortion due to the clipping process that performed iteratively until PAPR threshold is achieved. However, this is not same as normal clipping [4][5] because the subtraction of peak that over the PAPR threshold with the original signal is done in frequency domain, not in time like usual clipping technique. This technique provide better BER performance and does not introduce spectrum broadening which is usually arises on clipping in time domain. This technique was introduced in [15] and other method but still similar is in Armstrong method [16][17] and peak cancellation [18].

However, the cost of getting minimum BER degradation and system without spectrum broadening must be paid by increasing the amount of calculation. One iteration process increases the calculation of IFFT/FFT two times. This increasing is linear to the iteration times.

Our investigation on this technique confirms that for achieving a level of PAPR need more than 3 iterative processing. Because of the number of iterations is large, the BER performance will degrade larger.

4.1 Transmitter Structure

Fig. 4.1 describes the transmitter structure of OFDM with IP method. Modulated data are converted from serial to parallel, and then it is transformed to OFDM symbols in time domain by IFFT. The peak power components which exceed permission PAPR in each OFDM symbol are detected by peak detector to obtain $p(n)$

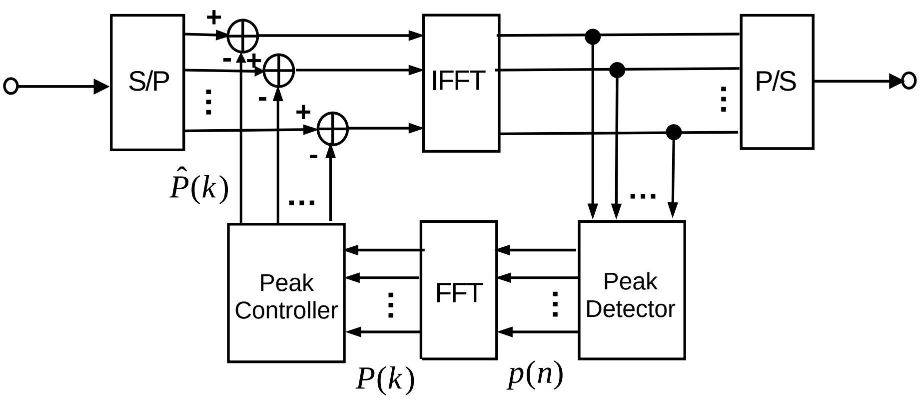

Fig. 4.1 Iterative Processing Structure at the OFDM Transmitter

$p(n)$ is defined by

$$p(n) = \begin{cases} x(n) & |x(n)| \le \eta \\ x(n) - \dfrac{x(n)}{|x(n)|} \cdot \eta & |x(n)| > \eta \end{cases} \tag{4.1}$$

where *x(n)* is n-th sampling signal in each OFDM symbol, and η is the desired PAPR threshold. Signal $p(n)$ is then FFT-ed to obtain frequency domain peak cancellation signal $P(k)$ as

$$P(k) = \frac{1}{\sqrt{N}} \sum_{n=0}^{N-1} p(n) \exp\left(\frac{-j2\pi kn}{N}\right), (k = 0,1,2,\cdots, N-1) \tag{4.2}$$

Then peak cancellation signals P(k) which correspond to the virtual carrier are zeroed to obtain the frequency domain peak cancellation signal $\hat{P}(k)$. $\hat{P}(k)$ is then subtracted from a_k (a_k is the inputted modulated symbols), so that the peak generation is avoided. However, due to virtual carrier, the target PAPR lower bound can not be attained in single execution, therefore require iteration, as the name implies.

4.2 PAPR Performance

PAPR calculation conducted by computer simulation is plotted in Fig. 4.2. This graph is generated from 100,000 randomly distributed symbols with QPSK modulation and OFDM subcarriers are generated from FFT points of 128 and subcarriers numbers of 96 are used for data transmission while other 32 subcarriers are zeroed.

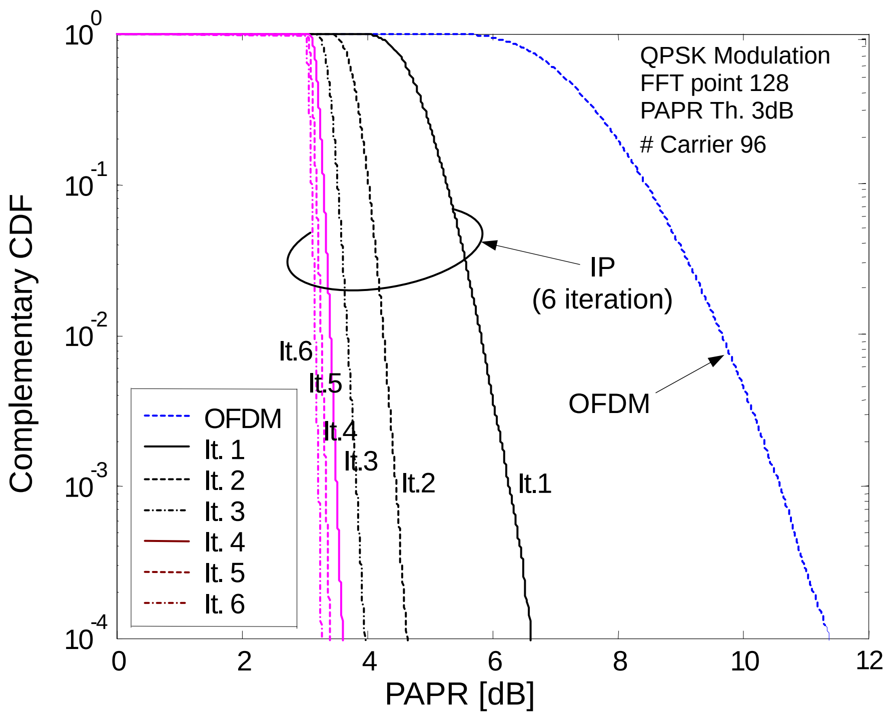

Fig. 4.2 OFDM PAPR Performance with Iterative Processing

From Fig. 4.2, PAPR resulted from the first iteration is 6.5dB, second iteration reduced to 4.5dB, third iteration results 4dB, and the 6th iteration approximately closed to the given threshold. it is clear that for achieving PAPR as given threshold, iterative processing has to be executed 6 times. It means there is addition of 6 x 2 = 12 times of IFFT/FFT calculations. We conclude this iteration time is still high and heavy.

4.3 BER Performance

Fig. 4.3 presents BER performance degradation of IP method with assuming the channel is AWGN. BER degradation depends on the iteration time, large iteration caused deep BER degradation. As shown in this figure, at BER of 10^{-4} we observe that the degradation is about 1dB, after three times iteration, total degradation becomes 2.8 - 3dB. This result shows that the BER degradation is still large when using IP method.

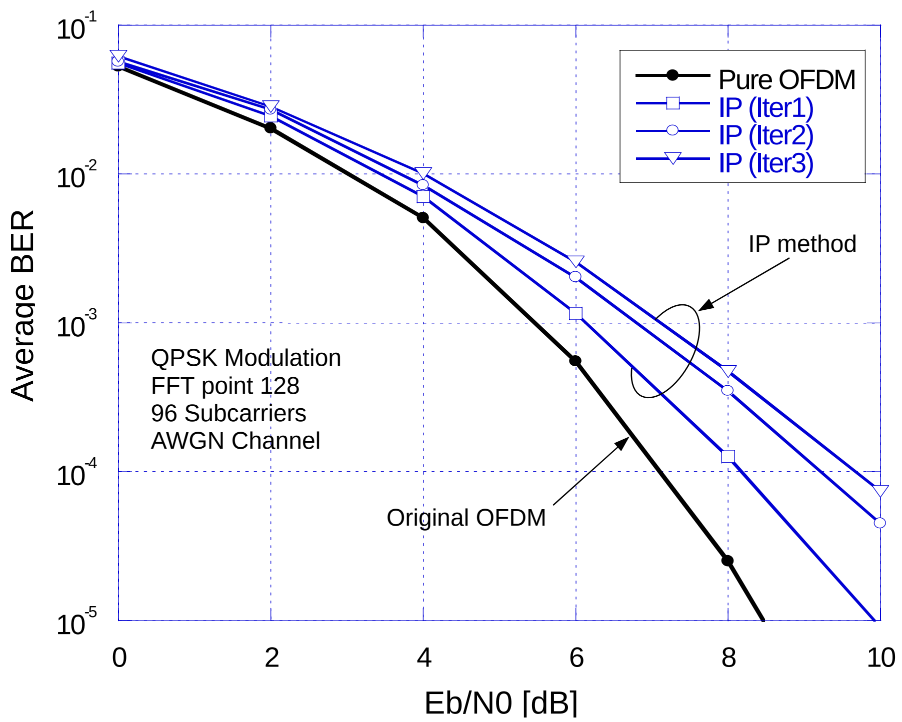

Fig. 4.3 BER Performance QPSK OFDM with Iterative Processing Method

4.4 Evaluations

With IP method, the number of iterative times is still large. It shall affect to: the serious increasing of the calculation amount makes the system heavy because of complex calculation of IFFT/FFT part; the large iteration time will make a deep degradation of the BER performance.

Due to this reason, there is a need for improvement related to these problems. It is possible to reduce significantly the iteration times, perhaps the number of iterations could be halved decreased.

Chapter 5

Proposed PAPR Reduction Method: Carrier Interferometry/Iterative Processing

Generally peak-to-average power ratio (PAPR) reduction method imposes transmission performance degradation or system capacity reduction. Two solutions for OFDM signals that have been analyzed in chapters 3 and 4 have some disadvantage, e.g., PAPR reduction is not significant, large amount of calculation and complexities, and large BER degradation.

This condition leads us to propose a new efficient method for reducing the PAPR of OFDM signals by combining carrier Interferometry (CI) spreading code and iterative processing (IP), called CI/IP [19]. This combining employed the advantages of CI in minimizing the high peak occurrence, and IP, which presented iterative clipping without out-of-band noise. This combination then results an efficient PAPR reductions technique and resulted new OFDM with high performance. The proposed method is capable of reducing the PAPR significantly while minimizing the bit error rate (BER) performance degradation. Computer simulation results prove the effectiveness of the proposed method. Further, the proposed method does not introduce out-of-band interference, which requires filtering whose complexity depends on the filtering requirement.

In this chapter, we describe the basic principle and idea of the proposed method in section 5.1, and then explanation of the proposed structure is provided in section 5.2.

5.1 The Basic Principle

The idea of the proposed technique is based on the principle that clipping the signals which has less peaks will provide better BER performance. CI codes is able to minimize the probability of high peaks, however, some peaks still appear because CI codes could not work perfectly in “cancelling” the IFFT/FFT process when partial subcarrier is considered. IP is then performed to clip the remaining peaks but the subtraction is carried out in frequency domain for obtaining clipping without spectral broadening.

For easy understanding, this principle illustrated in Fig. 5.1. This figure was generated from a randomly distributed 96 QPSK symbols. Then it is sent in pure OFDM and CI/OFDM and results in the OFDM signal and CI/OFDM signals as plotted in Fig. 5.1.

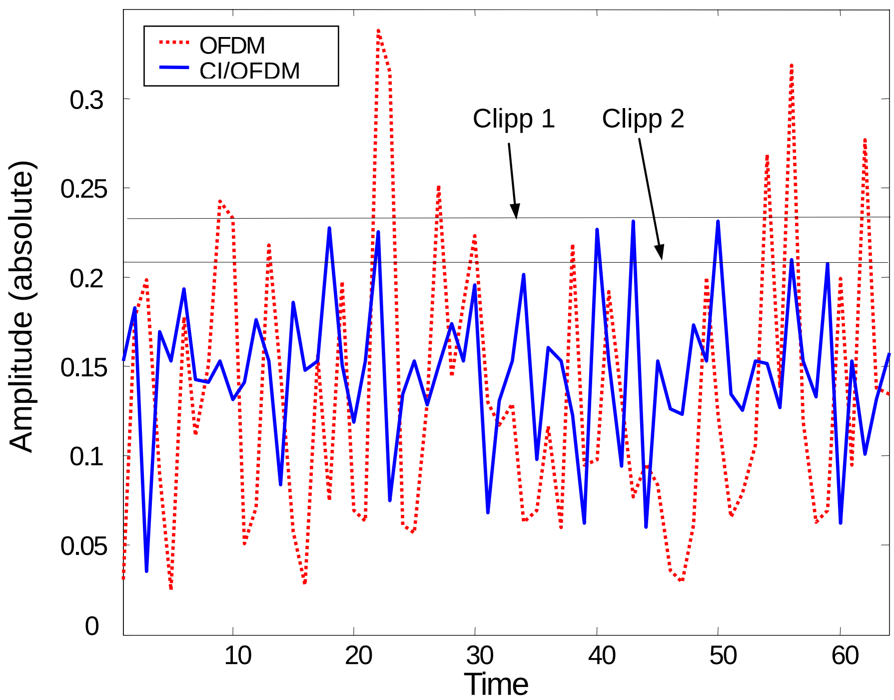

Fig. 5.1 Comparison of OFDM Symbol (dotted line) and CI/OFDM Symbol (solid line) with 128 IFFT Point and 96 Subcarriers

As shown in Fig. 5.1, OFDM signal has large peaks and CI codes minimize it and it results in the CI/OFDM with small number of peaks. With clipping level “clipp 1”(in IP term it is similar with the given PAPR threshold, even it is not completely same), there will be 6 peaks clipped, while no peak will be clipped using CI. It then affect the BER performance degradation, but no degradation when IP is utilized.

When the PAPR requirement is lower, clipping level or PAPR threshold can be set for example as “clipp 2”. In this case, the number of clipped peaks in OFDM signals is about 9 peaks with large distortion; while in CI/OFDM signals are only 5 peaks with small distortion. This fact will characterize CI/IP method has better BER performance degradation, reducing the iterative times and presented significant and lower PAPR performance.

5.2 Transceiver Structure

The structure of CI/IP method is presented in Fig. 5.2. Figure 5.2 (a) and (b) illustrate the block diagrams of OFDM transmitter and receiver, respectively, considered in this thesis. At the transmitter the information sequence to be transmitted is first QPSK data modulated then serial-to-parallel transformed before spreading with CI spreading codes. CI spreading codes for the *k*-th symbol is generated as (3.1) and [16]

$$CI_k = \left\{ e^{\{j(2\pi/N)\cdot k\cdot 0\}}, e^{\{j(2\pi/N)\cdot k\cdot 1\}}, \ldots, e^{\{j(2\pi/N)\cdot k\cdot (N-1)\}} \right\} \tag{5.1}$$

where N is the number of usable subcarriers. N generally is less than the FFT point N for practical reasons. Unlike binary valued orthogonal spreading codes, whose code length is generally restricted to the power of 2, CI spreading codes has no such restriction. Thus, offers flexibility to the system designer. Then, IFFT is performed to obtain time domain signal. CI reduces PAPR by avoiding the superposition of different information symbols in the time domain. Next, IP is performed on this output signal. First, peaks exceeding given threshold are detected to obtain peak signal

$$p(n) = \begin{cases} 0 & for\,|x(n)| \le \eta \\ x(n) - \dfrac{x(n)}{|x(n)|} \cdot \eta & for\,|x(n)| > \eta \end{cases} \tag{5.2}$$

where η is the desired PAPR threshold. *p(n)* is then FFT-ed to obtain frequency domain peak cancellation signal $P(k)$ as

$$P(k) = \frac{1}{\sqrt{N}} \sum_{k=0}^{N-1} p(n) \exp\left(\frac{-j2\pi kn}{N}\right), \quad (k = 0,1,...,(N-1)) \tag{5.3}$$

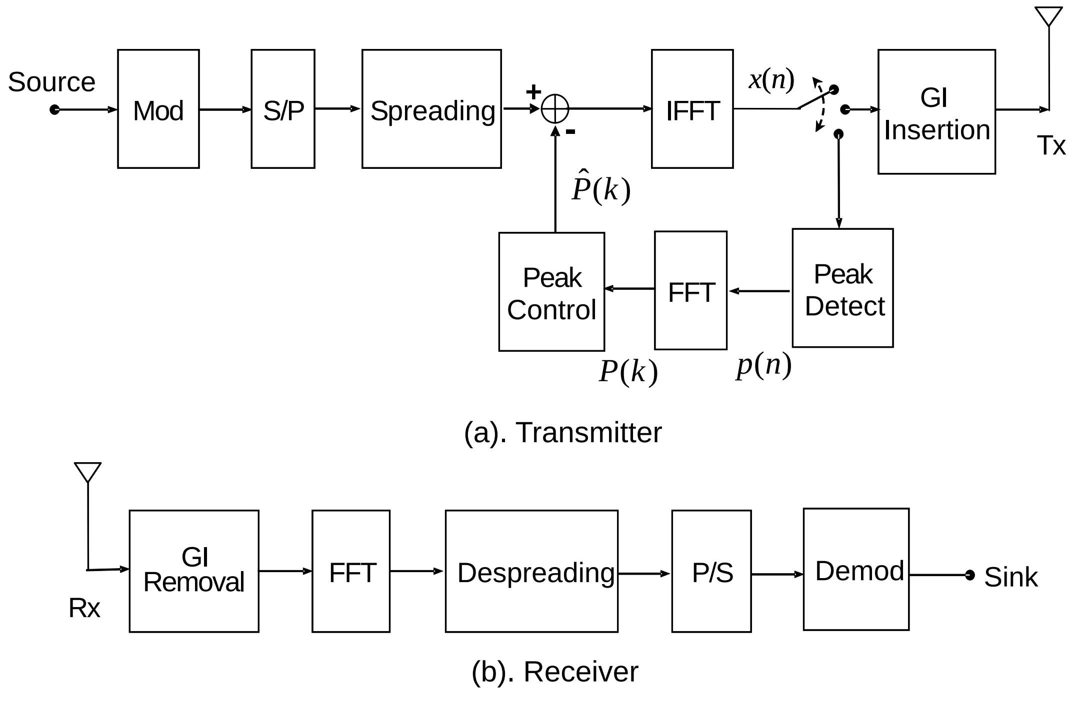

Fig. 5.2 Structure of Transceiver OFDM with the Proposed Method

Finally, peak cancellation signals $P(k)$ corresponding to the virtual carriers are zeroed to obtain the frequency domain peak cancellation signal $\widehat{P}(k)$. $\widehat{P}(k)$ is then subtracted from S_k (S_k is the result of multiplication between CI spreading codes and QPSK symbols) so that the peak generation is avoided. However, due to virtual carriers and average power decrease after IP, the target PAPR bound can not be attained in single execution therefore requires iteration; as the name implies. At the last stage of iteration, guard interval (GI) is inserted to produce the transmit signal. The transmit signal corrupted by AWGN is input to the receiver.

At the receiver, GI is first removed before FFT-ed to obtain the frequency domain signal. Despreading in the frequency domain and combining is performed before parallel-to-serial conversion followed by demodulation to recover the transmitted information sequence.

The combination of CI and IP for PAPR reduction has benefit of reducing iteration times when IP only is employed because CI alone reduces the PAPR of OFDM signal prior to applying iterative processing. Further, it also minimizes the BER degradation because of lesser distorted signal. Numerical result for this method is presented in chapter 6.

Chapter 6

CI/IP Performance Evaluations

This chapter presents the numerical result of the proposed CI/IP method. We performed computer simulations to clarify the performance of the proposed combination. There are three criteria that will be investigated in these evaluations: PAPR distribution, BER performance and power spectral density (PSD).

The major simulation parameters are shown in Table 1. In the simulation, we excluded the use of channel coding because it does not affect the PAPR distribution. Although the adoption of channel coding improves the BER performance, it does not fill the performance gap due to the distortion introduced by PAPR reduction techniques. PAPR characteristics are independent of generic forward error correction (FEC) coding thus their evaluation can be completely separated.

In [20], it has been demonstrated that the position of virtual carriers does not affect the PAPR characteristics or the system performance. In the simulation we placed the virtual subcarriers at the center of FFT bins.

Some part of this result has been presented in [19]. However, the results in this thesis have been extended to the investigation with lower PAPR threshold, i.e., 1dB and evaluation of BER performance degradation for this new PAPR threshold. For making a good comparison, PAPR of CI/IP method is plotted together with the PAPR of CI and IP solely.

TABLE 6.1

SIMULATION PARAMETERS FOR CI/IP METHOD

<table>
<tr><td rowspan="6">Transmitter</td><td>Modulation</td><td>QPSK</td></tr>
<tr><td>Spreading Code</td><td>Carrier Interferometry</td></tr>
<tr><td>Number of Subcarriers</td><td>96</td></tr>
<tr><td>FFT Point</td><td>128</td></tr>
<tr><td>PAPR Threshold</td><td>3dB, 1dB</td></tr>
<tr><td>Channel Coding</td><td>Off</td></tr>
<tr><td>Channel</td><td colspan="2">AWGN</td></tr>
<tr><td rowspan="2">Receiver</td><td>Channel Estimation</td><td>Off</td></tr>
<tr><td>Equalization</td><td>Off</td></tr>
</table>

6.1 PAPR Performance

Fig. 6.1 shows the complementary cumulative distribution function (CCDF) of the proposed PAPR reduction method (with threshold 3dB), i.e. combination of CI spreading codes and IP compared to that of using IP and CI. Fig. 6.2 then presents for the PAPR threshold of 1dB. We used 100000 randomly distributed symbols to produce both of the graphs. However, increasing the number of symbols beyond the value shall not drastically change the curves. CCDF of OFDM without any modification (hereafter called pure OFDM) is also shown for baseline comparison.

As shown in Fig. 6.1, PAPR at CDF of 99.90% performed by CI is about 7.5dB, IP iteration one is 6.3dB and the proposed method with iteration one is about 4.5dB. With iteration three, IP perform the PAPR about 3.8dB while proposed method is about 3dB at the same CDF of 99.90%. IP is able to achieve the same PAPR performance as CI/IP when the number of iteration is six, as presented in Fig. 4.2. It means that the proposed method is superior to IP method that halved the number of iterations required to attain the same given PAPR threshold. It then impacts on the reduction of the calculation amount that is also halved.

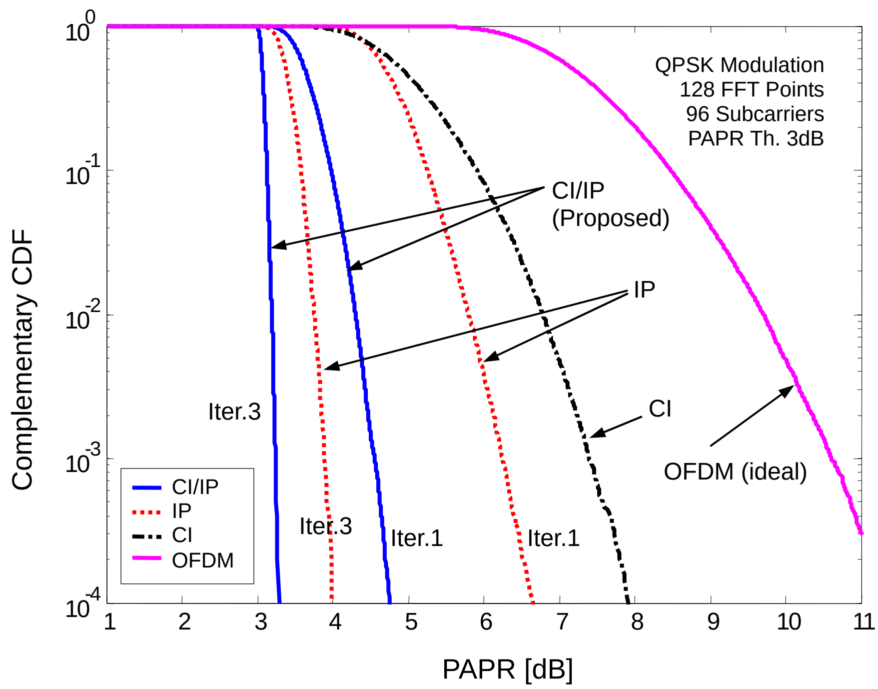

Fig. 6.1 OFDM PAPR Performance with CI/IP Method (Threshold=3dB)

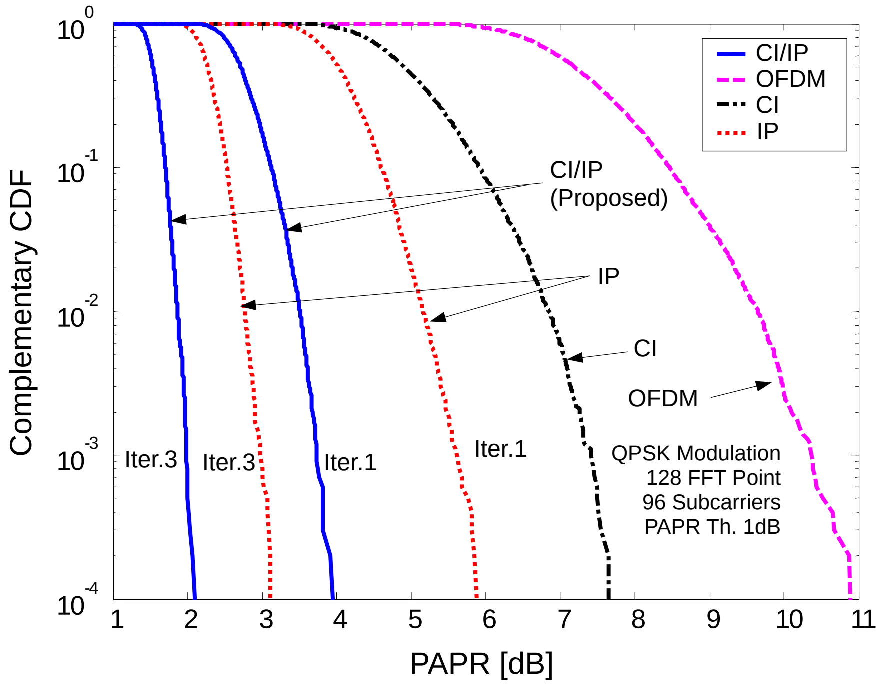

Fig. 6.2 OFDM PAPR Performance with CI/IP Method (Threshold=1dB)

Fig. 6.2 plots the result of the simulation with the PAPR threshold of 1dB. Threshold 1dB is selected for investigating how deep the reduction can be performed and how deep the BER degrades. Taking threshold > 3dB will not give any insight, because the lower the PAPR is the better.

With iteration one and CDF of 99.90%, IP achieved 5.5dB, while the proposed method achieved 3.8dB. With iteration three, IP reduces the PAPR to about 3dB while the proposed method is 2dB. It can be concluded that the proposed CI/IP is always better than IP solely. CI/IP is capable of showing lower PAPR with the small iteration. Consequently, the calculation amount is also significantly reduced.

6.2 BER Performance

We evaluated the BER degradation of the proposed method assuming AWGN channel as a function of received E_b/N_0. The results are plotted in Fig. 6.3 for PAPR threshold of 3dB and Fig. 6.4 for PAPR threshold of 1dB. At average BER of 10^{-4} we observe that the degradation of the proposed method after three iterations is within 1dB. On the other hand, the degradation with IP is about 3dB.

In Fig. 6.4 BER performance evaluation is presented for PAPR threshold of 1dB. At average BER of 10^{-3}, we observe that the degradation of the proposed CI/IP after three iterations is 2.5dB. At the same BER level, degradation of IP is approximately 8.5dB.

The proposed CI/IP method always performs better BER performance on any case of PAPR threshold. This can be explained as follows. Spreading by the CI codes reduces the PAPR so that the probability of a distortion introduced by the IP is decreased quite markedly.

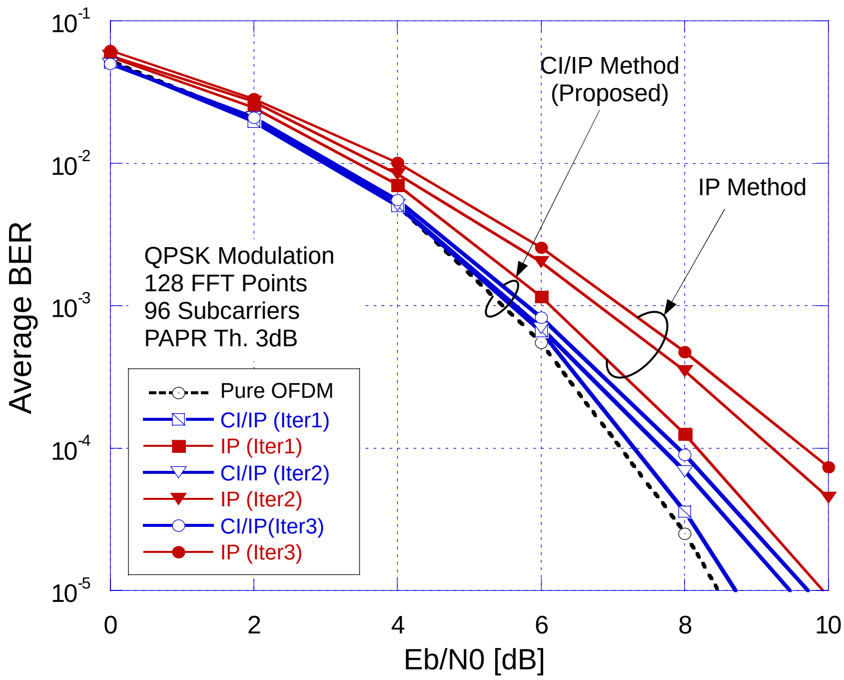

Fig. 6.3 Improvement of BER Performance Using CI/IP Method (Threshold=3dB)

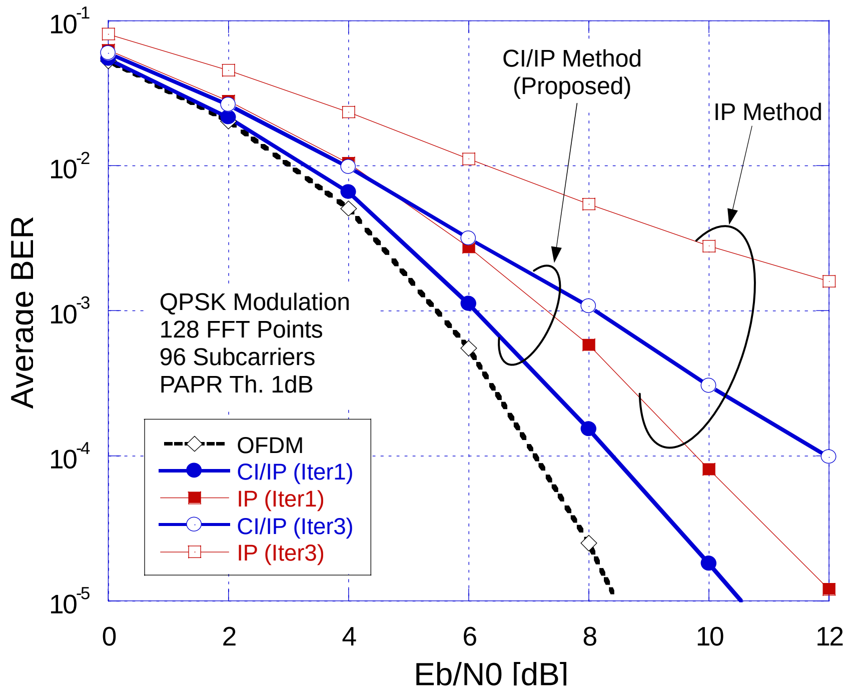

Fig. 6.4 Improvement of BER Performance Using CI/IP Method (Threshold=1dB)

6.3 Power Spectrum Density

Finally, we observed the power spectrum density (PSD) of the proposed method and compare it with the others. We assume that high power amplifier (HPA) at the transmitter has input back-off (IBO) larger than PAPR threshold, e.g., IBO = 5 or 6dB, while the proposed PAPR method obtains PAPR level equal to 2dB and 3dB. With this assumption, it is possible to check whether the proposed method is capable of presenting PSD as the original or affecting spectrum broadening that requires a complex filter.

Fig. 6.5 shows the average PSD of 500 OFDM symbols. From the figure it is evident that both IP and the proposed method retain the PSD of pure OFDM system as expected. This is due to the fact that the peaks cancellation signals are just valid OFDM signals.

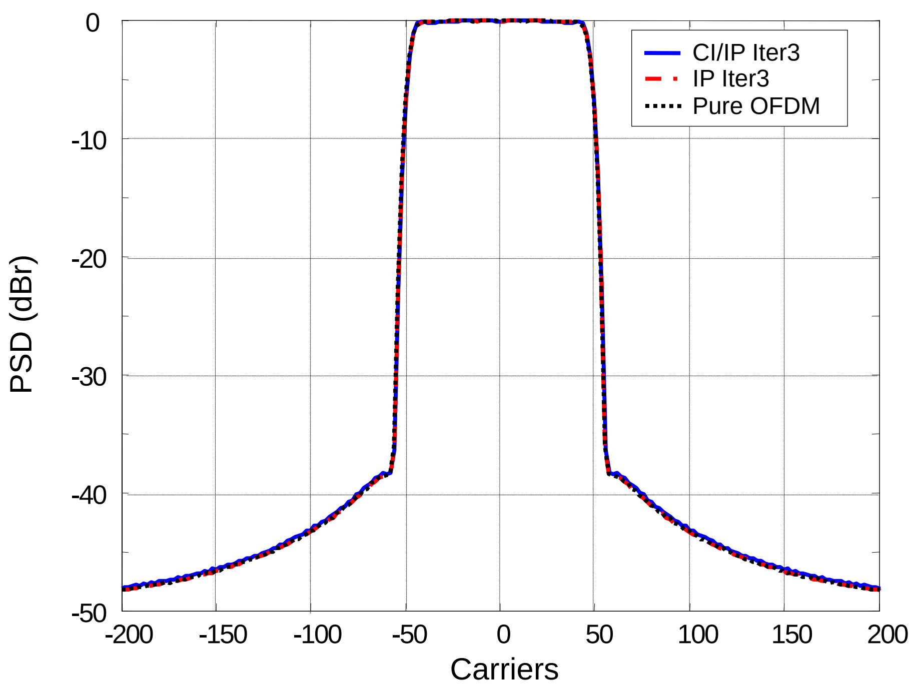

Fig. 6.5 Power Spectral Density of OFDM with IP and CI/IP Method

(no spectrum broadening)

Chapter 7

Thesis Summary and Conclusions

7.1 Thesis Summary

This thesis formulated the PAPR problem on OWDM system, OFDM system and proposed two new methods for PAPR reduction. Investigation on the orthogonality of PO-CI codes was also presented in detail.

Chapter 2 introduced the basic of multicarrier system and PAPR calculation. Then, PAPR for OFDM and OWDM is presented, and it is concluded that this PAPR of approximately 12-13dB, is still high and required to be reduced. For the case of OWDM system, orthogonal code i.e. Golay Complementary, CI, and Hadamard code are discussed to reduce PAPR of this system. We also showed the comparison with the PAPR of OFDM system. According to demonstration, Hadamard code outperforms CI and Golay complementary due to minimum superposition among the sub-channel. Demonstration using CCDF evaluation, oversampling, and amplitude limitation also has been presented. However, Hadamard code always offers better performance among others even with OFDM/CI in case of oversampling case.

The secret reason why Hadamard in OWDM and CI in OFDM exhibit low PAPR has been clarified. Low PAPR is achieved due to minimum superposition among the signal of any subcarriers. Therefore, to reduce the PAPR for wavelet based multicarrier modulation system, which is based on Haar wavelet, we propose the use of Hadamard code as the spreading code for the better performance.

Future work will be extended to wavelet with higher coefficient e.g. Daubechies wavelet family that has longer coefficients than Haar wavelet. Then investigate the code (new code), which has the "inverse" characteristic of wavelet filter utilized. Evaluation of its performance on fading environments is also our great interest.

Chapter 3 evaluated the PAPR of CI and PO-CI codes in OFDM system both when utilizing all and partial subcarriers for data transmissions. CI/OFDM PAPR when partial subcarrier is utilized for data transmissions, are only enabled PAPR reduction by approximately 2dB from the original. Analysis of imperfect orthogonality of PO-CI code was also evaluated in detail. It impacts the large number errors on M-QAM modulation because of the imperfect orthogonality which mainly on imaginary part are still remains even N is large. It makes PO-CI work only for BPSK and not longer efficient for M-QAM modulation. BER performance on various modulations was then described in the last part of this chapter.

In **Chapter 4**, Iterative Processing method was summarized. Iterative Processing is one kind of clipping technique that does not introduce out-of-band noise and possible to present lower BER degradation of OFDM system. However, the number of iteration is still large. It shall impact the increasing the amount of calculation and BER performance degradation.

Chapters 5 and 6 proposed an efficient method for PAPR reduction by combining CI and IP, which then called CI/IP method. The basic principle and transceiver structure is explained in chapter 5, while chapter 6 presented the proof by showing the numerical results. In the proposed method, transmit symbol sequence is spread using CI spreading codes prior to applying IP. The proposed combination significantly reduces the PAPR of OFDM signal. Interesting properties of the proposed method are that no out-of-band interference or spectral splatter is introduced and minimum BER degradation with respect to the ideal case. The proposed method also halved the number of required iterations to achieve the desired PAPR bound. Optimization to further reduce the iteration times requires further investigation in order to shrink the processing delays. Analysis on peak re-growth and higher order modulations are deferred to future investigation.

7.2 Conclusions

In this thesis, we evaluated the PAPR problem on multicarrier system especially OWDM and OFDM. For OWDM which is based on Haar wavelet, we proposed the use of Hadamard spreading codes to reduce its PAPR. Then we focus on the reduction of PAPR in OFDM system.

For OFDM signals, we have proposed the new efficient method by combining CI spreading code and Iterative processing. The proposed method is able to reduce PAPR significantly with the small number of iteration. This method also presented minimum BER performance degradation and does not introduce spectral broadening.

Future researches are addressed to the correction of PO-CI codes, starting from the restructuring imaginary part. Then distortion canceller should be employed in order to improve the BER performance of CI/IP method near to the original.

Acknowledgements

First of all and foremost, I thank to the God for His bless and merciful throughout all of my life. I also have many people to thank for helping to make my Nara experience both enriching and rewarding.

First, I would like to express my profound gratitude to Professor Heiichi Yamamoto, for his guidance and valuable support during my stay at Nara. His encouragement has been the most valuable throughout my studies at Nara.

I would like to thank to Associate Professor Minoru Okada for the valuable ideas, discussion and research guidance. My acknowledgements are also to Professor Hiroyuki Seki for his time of guiding me in writing this thesis.

I would like to express my gratitude to Associate Professor Takao Hara, for his outstanding guidance and limitless patient and fatherly support during my study and research. Prof. Hara is a fascinating teacher, thoughtful mentor and I benefited greatly working under his guidance.

I would like to thank to Associate Professor Masato Saito, for excellent technical discussion throughout all of my academic activity at Nara Institute of Science and Technology.

I would like to thanks to Dr. Akhmad Unggul Priantoro, International Islamic University of Malaysia, for some excellence ideas, ‘how to be good scientist’ and very valuable technical discussions during our stay in Nara Institute of Science and Technology, Japan.

I would like to thank the Panasonic Scholarship Inc., Japan, for giving me a chance to pursue my studies in Japan, valuable help and support during my stay at Japan.

Finally, I'll give my acknowledgements to all my friends from Japan or abroad, my present and past member of Communications Laboratory, who helped creating a very enjoyable and productive environment in the laboratory.

Through it all, I owe my greatest debt to my family – my parents, my wife and children. Your love, patient and support are the most rewarding experience of my graduate years.

References

[1] R. V. Dalal, *Orthogonal wavelet division multiplexing (OWDM) for broadband wireless communication*, A Master Thesis of University of South Florida, August 1999.

[2] G. Strang and T. Nguyen, “Wavelet and Filter Banks”, Wellesley, Cambridge, 1997.

[3] M. Vetterli and J. Kovacevic, “Wavelet and Subband Coding”, Prentice Hall, 1995.

[4] X. Li. and J. Cimini Jr., “Effect of clipping and filtering on the performance of OFDM,” *Proc. IEEE Vehicular Tech. Conference*, pp. 1634-1638, May 1997.

[5] H. Ochiai and H. Imai, “On clipping for peak power reduction of OFDM signals”, *IEEE Globecom’00, Vol. 2*, 2000, pp. 731-735.

[6] C. R. Nassar, B. Natarajan, Z. Wu, D. Wiegandt, S. A. Zekavat and S. Shatill, “Multi-carrier technologies for wireless communication”, Kluwer Academic Publishers, 2002, chapter 3-6.

[7] K. Anwar, A.U. Priantoro, M. Saito, T. Hara, M. Okada and H. Yamamoto, “On the PAPR reduction for wavelet based transmultiplexer”, *Proc. IEEE International Symposium on Communications and Information Technology (ISCIT2004)*, Sapporo, Japan, October 2004, pp. 812-815.

[8] K. Anwar, A.U. Priantoro, M. Saito, M. Okada and H. Yamamoto, “On the PAPR reduction for wavelet based multicarrier modulation system”, *Proc. IASTED*

International Conference on Communications and Computer Network (CCN2004), MIT, Cambridge, USA, November 2004, pp. 138-143.

[9] K. Brüninghaus and H. Rohling, “Multi-carrier spread spectrum and its relationship to single-carrier transmission”, *IEEE Vehicular Tech. Conf. ’98*, 1998, pp. 2329-2332.

[10] D. A. Wiegandt, C. R. Nassar and Z. Wu, “Overcoming Peak-to-Average Power Ratio Issues in OFDM via Carrier Interferometry Codes”, *IEEE Vehicular Technology 2001-Fall (VTC2001-Fall),* October 2001.

[11] D. A. Wiegandt, Z. Wu and C. R. Nassar, “High-throughput, High Performance OFDM via Pseudo-Orthogonal Carrier Interferometry Spreading Codes”, *IEEE Transaction on Communications*, *Vol. 51*, *No. 7,* July 2003.

[12] B. Natarajan, Z. Wu, C. R. Nassar, “Large Set of CI Spreading Codes for High Capacity MC-CDMA”, *IEEE Transaction on Communications*, *Vol. 52*, *No. 11*, November 2004.

[13] K. Anwar, M. Saito, T. Hara, M. Okada and H. Yamamoto, “Impact of using partial number subcarrier on the PAPR carrier interferometry OFDM”, *IEICE General Conference 2005*, Osaka, Japan, March 2005.

[14] M. Saito, K. Anwar, T. Hara, M, Okada and H. Yamamoto, “Effect of imperfect orthogonality PO-CI codes on the performances of M-QAM OFDM and MC-CDMA System”, *IEICE General Conference 2005,* Osaka, Japan, March 2005.

[15] S. Tomisato, H. Suda and M. Hata, “PAPR reduction method using iterative processing for OFDM transmission systems,” *Proc. of the 1st IEEE VTS Asia Pacific Wireless Communications APWCS2004,* pp.7-10, January 2004.

[16] J. Armstrong, "Peak-to-average power reduction for OFDM by repeated clipping and frequency domain filtering", *Electronics Letters* Vol. 38, No.5, February 2002, pp 246-247.

[17] H. A. Suraweera, C. Chai, J. Shentu and J. Armstrong, "Analysis of impulse noise mitigation techniques for digital television systems", *8th International OFDM Workshop*, Hamburg, Germany, September 2003, pp. 172-176.

[18] R. Van Nee, and R. Prasad, “OFDM for Wireless Multimedia communications”, Artech House Publisher, 2000, chapter 6.

[19] K. Anwar, A. U. Priantoro, K. Ando, M. Saito, T. Hara, M. Okada and H. Yamamoto, “PAPR reduction of OFDM signals using iterative processing and carrier interferometry codes”, *Proc. IEEE International Symposium on Intelligent Signal Processing and Communications System (ISPACS2004),* Seoul, Korea, November 2004, pp. 48-51.

[20] H. Liu and U. Tureli, “A high efficiency carrier offset estimator for OFDM communications”, *IEEE Communications Letter* Vol. 2, April 1998, pp. 104-106.

Appendix

Covariance and Correlation

Covariance and correlation are closely related parameters that indicate the extend extent to which two random variables co-vary. Suppose there are two technology stocks. If the price of one rises, the price of the other is also likely to rise. If the price of one falls, the price of the other is also likely to fall. Because they are affected by the same industry trends, the two prices tend to co-vary. They have positive covariance and positive correlation.

Let's formalize this. Consider a random vector ***X*** whose components are random variables X_i:

$$\mathbf{X} = \begin{pmatrix} X_1 \\ X_2 \\ \vdots \\ X_n \end{pmatrix} \tag{A.1}$$

Given any pair of components, X_i and X_j, we denote their covariance as either $\mathrm{cov}(X_i, X_j)$ or $\Sigma_{i,j}$. The covariance is defined by the expectation

$$\mathrm{cov}(X_i, X_j) = E\left[(X_i - \mu_i)(X_j - \mu_j)\right] \tag{A.2}$$

where μ_i and μ_j are the means of X_i and X_j. By definition, covariance is symmetric, with $\Sigma_{i,j} = \Sigma_{j,i}$. Also, the covariance of any component X_i with itself is that component's variance:

$$\operatorname{cov}(X_i, X_i) = E\left[(X_i - \mu_i)^2\right] = \operatorname{var}(X_i) \tag{A.3}$$

We summarize all the covariances of a random vector X with a covariance matrix:

$$\Sigma = \begin{pmatrix} \Sigma_{1,1} & \Sigma_{1,2} & \Sigma_{1,3} & \cdots & \Sigma_{1,n} \\ \Sigma_{2,1} & \Sigma_{2,2} & \Sigma_{2,3} & \cdots & \Sigma_{2,n} \\ \Sigma_{3,1} & \Sigma_{3,2} & \Sigma_{3,3} & \cdots & \Sigma_{3,n} \\ \vdots & \vdots & \vdots & \ddots & \vdots \\ \Sigma_{n,1} & \Sigma_{n,2} & \Sigma_{n,3} & \cdots & \Sigma_{n,n} \end{pmatrix} \tag{A.4}$$

Due to the symmetry property of covariances, this is necessarily a symmetric matrix. It can be shown that covariance matrices are positive definite of positive semidefinite.

The magnitude of a covariance $\Sigma_{i,j}$ depends upon the standard deviations of two components X_i and X_j. To obtain a more direct indication of how two components co-vary, we scale covariance to obtain correlation.

Given any pair of components, X_i and X_j, we denote their correlation as either *cor(*X_i*,* X_j*)* or $\rho_{i,j}$. The correlation is defined as

$$\rho_{i,j} = \frac{\operatorname{cov}(X_i, X_j)}{\sigma_i \sigma_j} \tag{A.5}$$

where σ_i and σ_j are the standard deviations of X_i and X_j.

By construction, a correlation is always a number between -1 and 1. Correlation inherits the symmetry of covariance: $\rho_{i,j} = \rho_{j,i}$. From (A.3) and (A.5), $\rho_{i,i} = 1$, which indicate that a random variable co-varies perfectly with itself. If X_i and X_j are independent, their correlation is 0. the converse is not true. As with covariances, we can summarize all the correlations of a random vector X with a symmetric correlation matrix:

$$\rho = \begin{pmatrix} \rho_{1,1} & \rho_{1,2} & \rho_{1,3} & \cdots & \rho_{1,n} \\ \rho_{2,1} & \rho_{2,2} & \rho_{2,3} & \cdots & \rho_{2,n} \\ \rho_{3,1} & \rho_{3,2} & \rho_{3,3} & \cdots & \rho_{3,n} \\ \vdots & \vdots & \vdots & \ddots & \vdots \\ \rho_{n,1} & \rho_{n,2} & \rho_{n,3} & \cdots & \rho_{n,n} \end{pmatrix} \tag{A.6}$$

List of Published Papers

International Conferences

1. K. Anwar, A. U. Priantoro, K. Ando, M. Saito, T. Hara, M. Okada and H. Yamamoto, "PAPR Reduction of OFDM Signals Using Iterative Processing and Carrier Interferometry Codes", *IEEE International Symposium on Intelligent Signal Processing and Communications System* (ISPACS2004), pp. 48-51, Seoul, Korea, November 2004.
2. K. Anwar, A. U. Priantoro, M. Saito, T. Hara, M. Okada, H. Yamamoto and K. Ando, "Digital Television Transmission over OFDM/FM Using Satellite Communications System", *IASTED International Conference on Communication, Internet and Information Technology* (CIIT2004), pp. 358-363, St. Thomas, Virgin Island, USA., November 2004.
3. K. Anwar, A. U. Priantoro, M. Saito, M. Okada and H. Yamamoto, "On the PAPR Reduction of Wavelet Based Multicarrier Modulation System", *IASTED International Conference on Communications and Computer Networks* (CCN2004), pp. 138-143, MIT, Cambridge, USA, November 2004.
4. K. Anwar, A. U. Priantoro, M. Saito, T. Hara, M. Okada and H. Yamamoto, "On the PAPR Reduction of Wavelet Based Transmultiplexer", *IEEE International Symposium on Communications and Information Technology* (ISCIT2004), pp. 812-815, Sapporo, Japan, October 2004.
5. K. Ragab, N. Kaji, K. Anwar, Y. Horikoshi, H. Kuriyama and K. Mori, "A Novel Hierarchical Community Architecture with End-to-End Delay Awareness for Communications Delay Enhancement", *IEEE International Symposium on Application and the Internet* (SAINT2004), pp. 43-49, Tokyo, Japan, January 2004.

Local Conferences

1. K. Anwar, M. Saito, T. Hara, M. Okada and H. Yamamoto, "Impact of Using Partial Number of Subcarrier on the PAPR Carrier Interferometry OFDM", *IEICE General Conference 2005*, Osaka, March 2005.
2. M. Saito, K. Anwar, T. Hara, M. Okada and H. Yamamoto, "Effect of Imperfect Orthogonality PO-CI Codes on the Performances of M-QAM OFDM and MC-CDMA System", *IEICE General Conference 2005*, Osaka, March 2005.
3. K. Anwar, A. U. Priantoro, M. Saito, T. Hara, M. Okada and H. Yamamoto, "On the PAPR Reduction for Wavelet Based Multicarrier Modulation", *Indonesian Scientific Forum* (TI2004), Tokyo, September 2004.
4. K. Anwar, K. Ragab and K. Mori, "Autonomous Decentralized Sensor Network and Its Application on ITS", *Indonesian Scientific Forum* (TI2003), Osaka, July 2003.
5. K. Anwar, Ian Y. M., and Hendrawan, "Interoperability of Digital Switching System (5ESS, EWSD, NEAX61E) on the Implementation of Signalling System No. 7", *Indonesian Scientific Forum* (TI2002), Nagoya, September 2002.